J. Phys. A: Math., Nucl. Gen., Vol. 6, July 1973. Printed in Great Britain.

Special features of high energy hadrons in air showers

R H Vatcha and B V Sreekantan

Tata Institute of Fundamental Research, Bombay-5, India

Received 7 December 1972

Abstract. The properties of hadrons of energy $2{\cdot}5 \times 10^{10}$–10^{13} eV in air showers of size 5×10^4–3×10^6 particles at 800 g cm^{-2} have been studied using a 2 m^2 multiplate cloud chamber as the hadron detector operated at the centre of the TIFR air shower array at Ootacamund. The results show a tendency for the lateral distribution of high energy hadrons to flatten with increasing shower size. The energy spectrum in the range 50–800 GeV steepens continuously with size and the number of hadrons does not increase linearly with size, but at a much slower rate especially for high energy hadrons. The fractional energy spectrum of hadrons of energies greater than 200 GeV is different for showers of size less than and greater than 3×10^5 particles. The charge to neutral ratio of hadrons of energy greater than 25 GeV in showers of size less than $3{\cdot}2 \times 10^5$ is found to have a rather low value ($6{\cdot}2 \pm 1{\cdot}3$) and there is evidence for a further decrease in this value for larger size showers. While a comparison of the present results with those of others is presented in this paper, the interpretation of the results in terms of primary composition and the characteristics of high energy interactions is reserved for two subsequent papers.

1. Introduction

With the advent of intersecting storage rings at CERN, it has now become feasible to extend observations on the characteristics of p–p collisions up to energies of the order of 2×10^{12} eV. However, there is considerable interest and need to know the behaviour of strong interactions at still higher energies especially from the point of view of the interpretation of cosmic ray phenomena at the highest energies and also for verifying the asymptotic validity of scale invariance theories (Feynman 1969). With the help of extensive air showers (EAS) it is possible to extend the study of the characteristics of strong interactions up to very high energies. The low flux of primary cosmic rays is compensated in EAS studies by large detection areas that become effective as a result of the spread of the secondary particles. However, due to the complexity of the air shower phenomenon, the interpretation of results is not straightforward. A major problem arises in distinguishing the effects of primary composition from those of collision characteristics. Several investigators have carried out detailed Monte Carlo simulations of air showers to identify features which are exclusively sensitive to either the mass of the primary nucleus initiating the shower or to the characteristics of ultra-high energy collisions. It has become apparent that it is only through a number of iterative stages of study of the correlations between the different components and the internal consistency in their behaviour that the complex effects of these two aspects can be segregated and knowledge concerning both gained. Among the various secondary components the two which are particularly sensitive to changes in primary composition and collision characteristics are the high energy hadrons which constitute the back-bone and skeleton of air showers and the ultra-high energy muons which arise predominantly in the first few collisions at the top of the atmosphere.

The situation concerning the experimental data on high energy hadrons in air showers is far from satisfactory. The high energy hadrons are concentrated in regions close to the core and their number is quite low. The hadron detector assemblies are necessarily complicated since they have not only to detect hadrons, but also measure their energy. Among the non-visual type of hadron detectors, transition chambers, ionization calorimeters and total absorption spectrometers have been used. These suffer the disadvantage that they do not enable the separation of charged hadrons from neutral ones, and events caused by the incidence of multiple particles from those caused by single hadrons. Multiplate cloud chambers offer a distinct advantage in this respect. However, there are very few experiments that have been carried out using cloud chambers. Besides there exists considerable disagreement between the results of different experiments using different types of detectors for studying the high energy hadrons in EAS (see, for example, Murthy 1967).

We have studied the properties of hadrons of energy greater than $2{\cdot}5 \times 10^{10}$ eV in air showers of size 5×10^4–3×10^6 particles using a 2 m^2 multiplate cloud chamber, at the centre of the Ooty air shower array. In this paper we present briefly the experimental details and the methods of analysis of data, and give a fairly comprehensive account of the experimental results that we have obtained and then make a comparison of the results with those of other experiments and point out certain special features in the variation with shower size of some properties of the high energy hadronic component. In accompanying papers we consider the interpretation of these results in the light of the Monte Carlo simulations that exist on the hadronic component of proton and heavy primary induced EAS and discuss the trends in the characteristics of strong interactions at ultra-high energies which are needed to explain the observed results.

2. Experimental details

The TIFR air shower array at Ooty (800 g cm^{-2}) which is designed for recording showers in the size range 5×10^4–5×10^6 particles is shown in figure 1. The full details are available elsewhere (Vatcha 1972). For individual showers in this size range the array provides information on the position of the axis, the shower size, the direction of arrival and also the value of the steepness parameter α_e, in the lateral distribution function of electrons given by

$$\Delta(r) = \frac{N_e}{2\pi r_0^2} \frac{\exp(-r/r_0)}{(r/r_0)^{\alpha_e}\Gamma(2-\alpha_e)}.$$

The values of core position, shower size and α_e are obtained by a χ^2 minimization procedure using a CDC-3600 computer. The direction of arrival is determined by the usual fast-timing technique.

The hadron detector located at the centre of the array is a large multiplate cloud chamber of dimensions 2 m × 1·5 m × 1 m with 21 iron plates inside, each of 2 cm thickness corresponding to a radiation length, and the whole plate assembly corresponds to about 2·2 interaction mean free paths. The chamber is shielded on the top by an absorber equivalent to about 5·5 radiation lengths of iron and lead.

The method of estimating the energy of hadrons interacting in the chamber has been described in detail in an earlier paper (Vatcha *et al* 1972). For cascade energies less than 200 GeV, it is feasible to count individual tracks and the energy is determined by evaluating the track length integral. For higher energy cascades a new method of

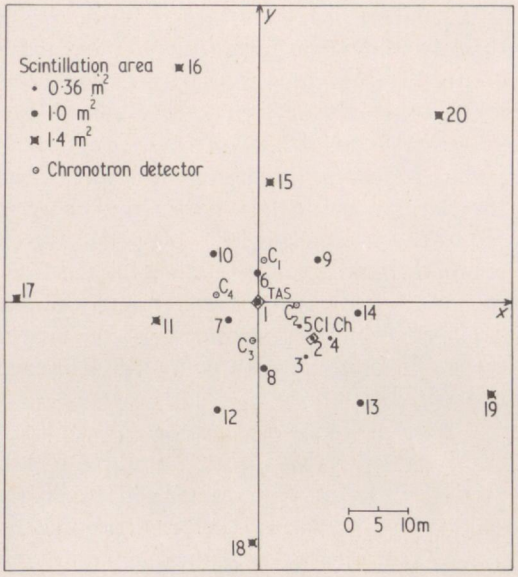

Figure 1. The extensive air shower array at Ootacamund.

evaluating the track length integral by measuring the 'saturated widths' of the cascades at different stages of development, and using Monte Carlo simulations for calibrations has been developed and used. The statistical error in the energy estimate of hadrons is better than 50% up to the highest energies. It has been shown elsewhere (Vatcha 1972) that due to some uncertainty in the measurements of saturated widths there may be a systematic underestimate of hadron energies. The maximum probable underestimate is about 50%.

The cloud chamber was operated in association with the air shower array from August 1968 to February 1969 and from November 1969 to September 1970. A total of 20 000 showers was recorded in an effective operation time of 6800 hours using different electron density criteria for air shower selection. The details regarding the operational features, the method of analysis of cloud chamber photographs, the classification of data, the selection criteria, evaluation of the 100% efficiency areas, the efficiency of the hadron detector for different angles of incidence and the evaluation of errors in the different parameters etc are available elsewhere (Vatcha 1972). The procedure used for evaluating the flux of hadrons automatically takes into account the effects of angular distribution of showers and is insensitive to the exact value of interaction mean free path of hadrons in iron. In addition to the cloud chamber, the total absorption spectrometer, TAS (located at a distance of about 11 m from the cloud chamber), described elsewhere (Ramana Murthy *et al* 1963) was also operated during the entire period as a second hadron detector and this enabled a comparison of data on hadrons from visual and non-visual detectors in the same experiment.

2.1. The lateral distribution of hadrons

For detailed analysis the size interval $5{\cdot}6 \times 10^4$–$5{\cdot}6 \times 10^6$ particles is divided logarithmically into 8 sub-intervals. The distance interval between the shower axis and the cloud chamber which extends mostly up to about 32 m is divided such that the Rth interval

extends from $2^{(R-1)/2}$ m to $2^{R/2}$ m. The hadron energy intervals are classified such that the nth interval extends from $25\times 2^{n-1}$ GeV to 25×2^{n} GeV. The steepness parameter is classified into 5 equal sub-intervals extending from 0 to 2·0. The density of hadrons per shower in any particular sub-group is given by

$$\Delta(N_e, r, >E_H) = \frac{H(N_e, r, >E_H)}{N(N_e, r)} F$$

where H is the observed number of hadrons in the bin of average size N_e, average distance r and hadron energy greater than E_H; N is the observed number of showers in the same bin and F is the geometrical factor of the cloud chamber.

The densities of hadrons obtained in this way were compared for different triggers to check the bias due to triggering inefficiencies at different core distances. No appreciable difference for the different triggers was found. This was further verified by calculating the average values of 'α_e' for different triggers and for different size and distance groups. Therefore data from all density triggers were combined to obtain the lateral distribution and some typical cases are plotted in figure 2 for hadrons of energies greater than 50 GeV

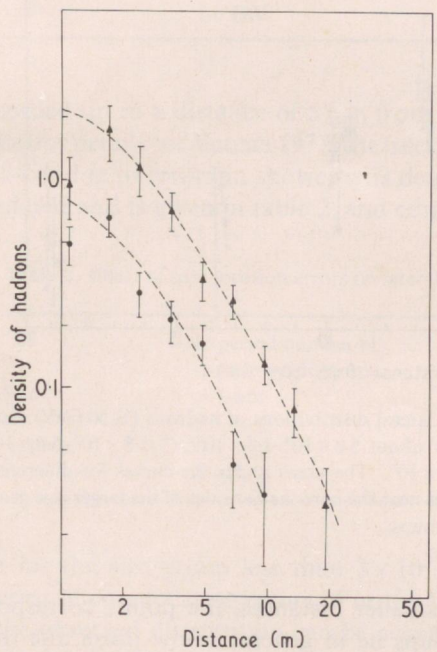

Figure 2. The lateral distribution of hadrons (> 50 GeV) associated with EAS in two typical size groups: $1{\cdot}8\times10^5$–$3{\cdot}2\times10^5$ (●) and 10^6–$1{\cdot}8\times10^6$ (▲). The broken curves are the best fits to the experimental points.

for two size regions. The distributions are similar at other sizes and energies. The experimental points are fitted using the formula

$$\Delta_n(r) = \frac{N_n}{2\pi r_n^2} \frac{\exp(-r/r_n)}{(r/r_n)^{\alpha_n}\Gamma(2-\alpha_n)}$$

where Δ_n is the hadron density at a distance r, N_n is the total number of hadrons for the

given shower size and α_n, r_n are two free parameters with α_n subject to $0 < \alpha_n < 2$. The χ^2 minimization is done in two stages; in the first stage α_n is fixed. The value of N_n is not seriously affected by small deviations in values of r_n and α_n since the χ^2 surface is very flat over a large range of coupled values of r_n and α_n. Values of N_n obtained in this way are compared with values of N_n within 20 m of the shower core obtained by adding contributions from different distance groups directly. N_n (total) and N_n ($\leqslant 20$ m) agree reasonably well at lower sizes but increasingly disagree at higher sizes. This implies that a larger fraction of hadrons lie outside 20 m at higher sizes or in other words, the lateral distribution of hadrons flattens with increasing size. This feature is illustrated in figure 3 where the lateral distributions are plotted normalized to a constant

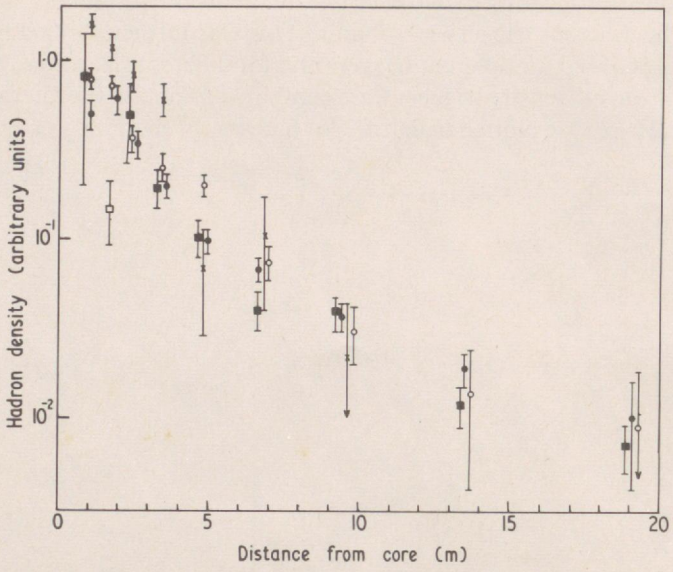

Figure 3. The normalized lateral distributions of hadrons (> 50 GeV) associated with EAS in different size groups: × about $5{\cdot}0 \times 10^4$–$1{\cdot}3 \times 10^5$; ○ $1{\cdot}8 \times 10^5$–$5{\cdot}6 \times 10^5$; ● $5{\cdot}6 \times 10^5$–$1{\cdot}8 \times 10^6$; ■ $1{\cdot}8 \times 10^6$–$5{\cdot}6 \times 10^6$. The areas under the curves for different size groups are normalized and at distances near the core the densities of the larger size groups are less than those of the smaller size groups.

N_n (total) for all size groups. At smaller distances, the points corresponding to the hadron densities in larger size groups lie in general below those due to smaller size groups. As the areas under the curves are normalized this again indicates a flattening of the lateral distribution with increasing size. Due to poor statistics it is difficult to make a quantitative evaluation of this trend.

2.2. Lateral distribution of cascades of energy greater than 1 TeV

During the 6800 hours of observation a total of 28 events due to hadrons of energies greater than 1 TeV were recorded in the chamber. Out of these 10 were associated with showers of size less than 3×10^5 and 18 with showers of size greater than 3×10^5. The lateral distribution of these events is given in table 1 and the energies of the individual hadrons are also listed. It is seen that hadrons with energies greater than a few TeV

Table 1. Lateral distribution of TeV cascades

Shower size \ Distance from core (m) r	0–1·4		1·4–2·0	2·0–2·8	2·8–4·0	4·0–5·6
$< 3 \times 10^5$	9/517		1/362	0/413	0/496	0/493
	1·8 TeV	2·0 TeV	1·5 TeV			
	2·2 TeV	2·5 TeV				
	70·0 TeV	150 TeV				
	9·0 TeV	2·5 TeV				
		2·5 TeV				
$> 3 \times 10^5$	11/176		2/182	2/275	2/490	1/788
	1·0 TeV	2·0 TeV	4·7 TeV	1·1 TeV	9·4 TeV	
	1·0 TeV	1·1 TeV	1·1 TeV	1·4 TeV	1·7 TeV	2·4 TeV
	2·0 TeV	2·6 TeV				
	3·5 TeV	2·6 TeV				
	1·4 TeV					
	9·0 TeV	15·0 TeV				
	1·0 TeV					

have been recorded up to a distance of 5·6 m from the core. On the basis of artificial shower analysis (for details see Vatcha 1972) the fraction of showers expected at distances greater than 1·4 m due to errors in shower axis determination for the two size groups has been calculated and is given in table 2, and compared with the observed fractions.

Table 2. Effect of core location errors on lateral distribution of TeV cascades

Size	Expected number of showers at distances $> 1{\cdot}4$ m	Observed number of showers at distances $> 1{\cdot}4$ m
$< 3 \times 10^5$	$(7 \pm 3)\%$	1/10
$> 3 \times 10^5$	$(7 \pm 2)\%$	7/18

It is seen that for the size group less than 3×10^5 the observed distribution can be explained in terms of core location errors. For the larger size group, however, it looks unlikely that the observed distribution can be accounted for in terms of core location errors, especially since in this case the distribution would fall off rather sharply. Whether these high energy events occurring at large distances from the core constitute evidence for large p_T will be discussed in a later paper.

2.3. The variation of the number of hadrons with size

The variation of the number of hadrons per shower as a function of shower size has been determined for different threshold energies of hadrons and is shown in figure 4. The hatched† areas represent the degree of uncertainty due to a possible systematic

† Henceforth this convention will be adopted.

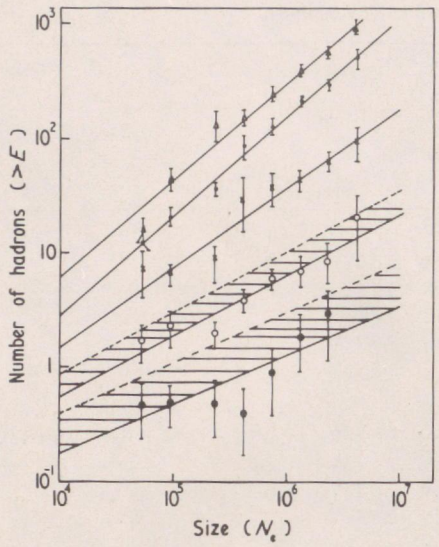

Figure 4. The variation of the number of hadrons of different energy thresholds 'E' with shower size. Values of E (GeV) are: 25; 50; 100; 200; 400. The straight lines are the least-square fits. The hatched regions pertaining to hadrons of energies greater than 200 GeV and greater than 400 GeV indicate the effects of a maximum probable underestimate in the energy of such hadrons.

underestimation in the hadron energy as described earlier. The full lines in the figure are the least-square fits to the equation

$$N_n(>E) = AN_e^{\alpha(E)}$$

in the size interval 5×10^4 to 3×10^6 particles. The results show an interesting trend. The *average* slope in this size region decreases with increasing hadron energy. It may be emphasized that any systematic error in the determination of the hadron energy can only change the value of the threshold energy but will not change the trend regarding the variation of $\alpha(E)$ with size, since the systematic error is not coupled to the size in the present cloud chamber experiment. In the case of experiments with non-visual hadron detectors, there could be a correlation between hadron energy estimate and shower size.

For hadrons of high energies there is even an indication of a break in the slope at a size $(3\text{–}4)\times10^5$. Below this size there is very little variation of N_n with N_e whereas the slope steepens above this size. The progressive flattening could be the result of such a break. It should be emphasized, however, that the statistical significance is not sufficient to claim a *definite* break on the basis of data for individual energy groups.

2.4. Integral energy spectra of hadrons (25–800 *GeV*)

The integral energy spectra of hadrons in the energy range 25–800 GeV in showers of size 7×10^4 to $3{\cdot}2\times10^6$ particles are given in figures 5(*a*, *b*). To provide clarity in the figures, the spectra for alternate size groups are plotted in parts (*a*) and (*b*).

In the energy range 50–800 GeV, the hadron spectra are represented by

$$N_n(>E) = BE^{-\gamma(N_e)}$$

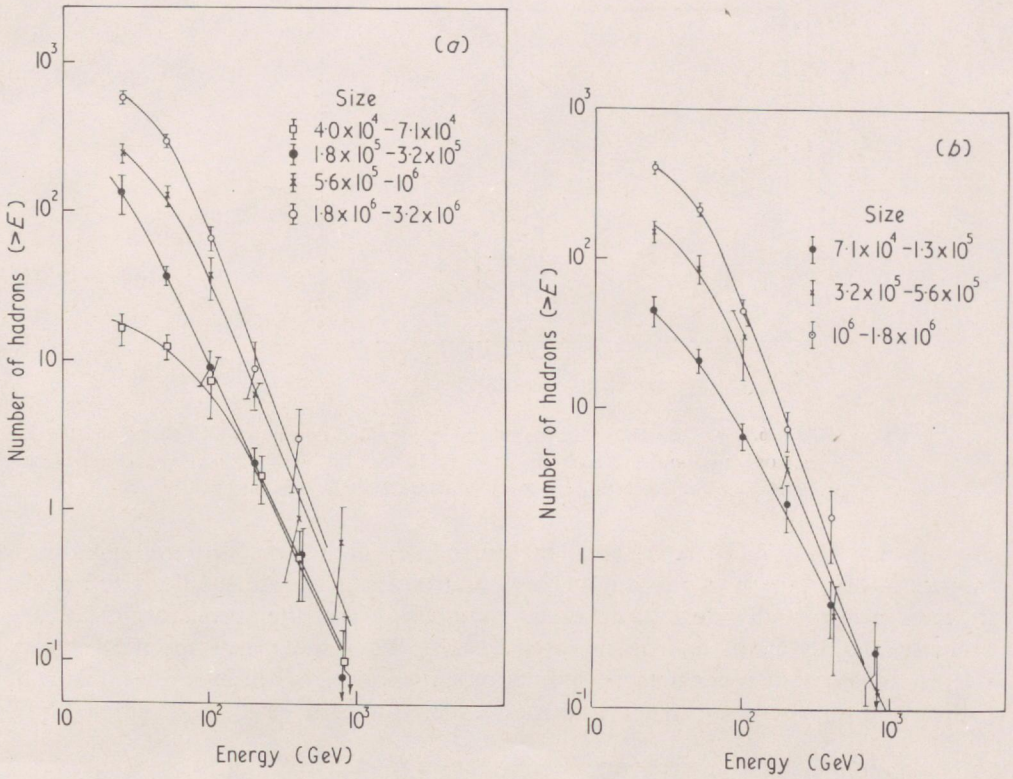

Figure 5. The integral energy spectrum of hadrons of energies from greater than 25 GeV to greater than 800 GeV associated with EAS of sizes ranging from 4×10^4 to $3{\cdot}2 \times 10^6$. For clarity alternate size groups are given in parts (*a*) and (*b*).

where the exponent γ is a function of shower size. The variation of γ with N_e is shown in figure 2 of paper III (curve A). It is seen that γ increases with N_e up to $3\text{–}4 \times 10^5$ particles and remains constant thereafter. Curve B in figure 2 of paper III is drawn after correcting for possible systematic underestimates of energy. It is seen that the tendency for γ to increase and flatten at a few times 10^5 is unaffected even after this correction.

There could be a slight bias in the experiment in determining the number of hadrons in the energy range 25–50 GeV in large air showers as some of these could be missed in the background of multiple high energy cascades. However the lateral distribution is flat enough for the total number not to be affected seriously. The variation of $\alpha(E)$ with E (§ 2.3) for showers in the size range 5×10^4–3×10^6 is shown in figure 6. It is seen that $\alpha(E)$, which has a value of about 0·8 up to 50 GeV, continuously decreases and has a value of about 0·4 at $E > 400$ GeV. The points with broken error bars are obtained after correcting for possible systematic errors in energy estimate. It is seen that this correction does not change the trend.

2.5. Energy spectra of very high energy hadrons

The very high energy events have been classified into only two size groups corresponding to average primary energies of about 3×10^5 GeV and approximately 2×10^6 GeV since the numbers are small. The averaged integral energy spectra for the two groups

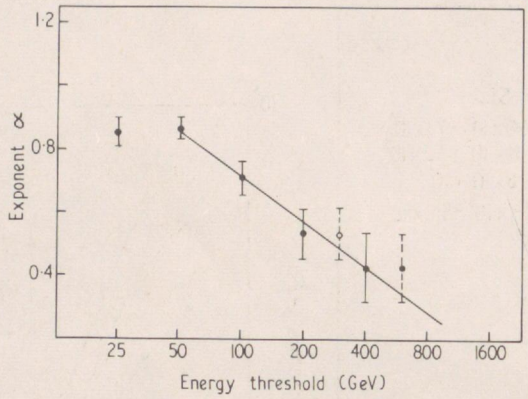

Figure 6. The variation with threshold energy of the exponent α which pertains to the size variation of the number of hadrons. $N_e = 5 \times 10^4$–5×10^6. The points with broken error bars are obtained after correcting for energy underestimate as explained before.

are shown in figure 7. There is a small bias introduced in the process of averaging since the lateral distribution of very high energy hadrons is steep and smaller size EAS are triggered preferentially close to the cloud chamber, so that the average weighted size decreases slightly as the hadron energy increases. When the energy spectrum is very steep it is essential to consider the effects of statistical errors in energy estimates of hadrons on the spectrum. If the true energy spectrum is given by $N_n\,(>E) = BE^{-\gamma}$,

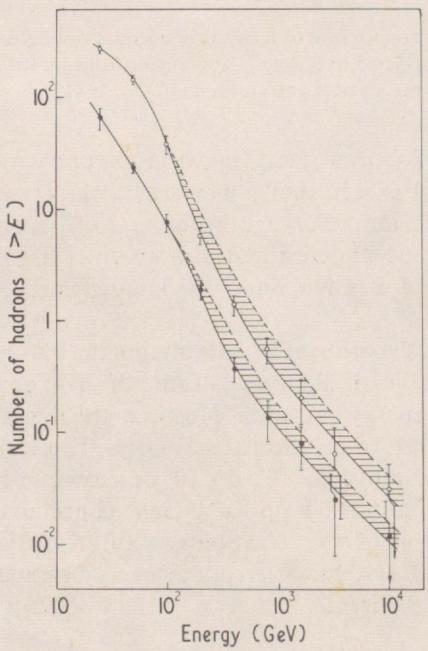

Figure 7. The integral energy spectrum of hadrons of energies from greater than 25 GeV to greater than 10 000 GeV associated with EAS of two size groups: ● $4{\cdot}0 \times 10^4$–$3{\cdot}2 \times 10^5$, average primary energy = 3×10^5 GeV; ○ $3{\cdot}2 \times 10^5$–$3{\cdot}2 \times 10^6$, average primary energy = 2×10^6 GeV. The hatched regions indicate the effects of energy underestimate as explained before.

then the observed spectrum would be as a result of statistical errors of the form

$$N_n(>E) = BE^{-\gamma}\{1-\beta+\tfrac{1}{2}\beta(2^{\gamma}+2^{-\gamma})\}$$

where β represents the fraction of hadrons transferred to the neighbouring energy channels (defined earlier) due to statistical errors in energy estimate. In deriving this relation, it is assumed that β is symmetrically distributed as is approximately indicated by the Monte Carlo simulations of hadronic cascades in the chamber (Vatcha 1972). In our case $\beta \simeq 0{\cdot}3$ to $0{\cdot}5$, and as γ approaches a value around 2, the actual number of hadrons $N_n(>E)$ may be smaller by about 35%. However, a detailed comparison of cascade profiles observed in the cloud chamber with those expected from Monte Carlo simulations has shown that the method adopted in obtaining hadron energies leads to a systematic underestimate by about 20% for hadrons of energies less than 200 GeV. Therefore we believe that this underestimate would approximately compensate for the statistical errors discussed above, and no corrections are necessary.

For energies greater than 800 GeV, the spectrum is averaged over all sizes and is approximately given by

$$N_n(>E) \sim E^{-1{\cdot}2}.$$

On integrating the energy spectrum of hadrons in an approximate manner, the percentage of the primary energy available in the hadronic component at 800 g cm^{-2} is found to be about 1·5% to 2·0% for $N_e < 3\times10^5$ and about 1·0% to 1·5% for $N_e > 3\times10^5$, the uncertainties arising from the shape of the spectrum at lower energies.

2.6. Fractional hadron energy spectrum

In figure 8 the integral energy spectra of hadrons of energy greater than 200 GeV are plotted for the same two size groups in a different way. The energy of the hadron is expressed as a fraction 'K' of the primary energy E_0 of the associated EAS. E_0 is calculated using the relation

$$E_0\,(\text{GeV}) = 2{\cdot}9\times10^6\left(\frac{N_e}{10^6}\right)^{0{\cdot}9}$$

where N_e is the number of electrons in the shower.

The number of hadrons per shower is obtained from the equation

$$N_n(>K) = F\sum_r \frac{T(r,>K)}{f(r)}$$

where F is the geometric factor of the cloud chamber, $f(r)$ is the observed flux per square metre of the showers at distance r and $T(r,>K)$ is the observed number of hadrons in the chamber of fractional energy greater than K at distance r from the core.

The experimental curves are compared with those expected for survivors of primaries calculated assuming different values of inelasticity and interaction mean free paths and different primary mass numbers. The detailed implications of such a comparison are discussed in paper II. The important point that we would like to stress at this juncture is that all sources of errors and biases tend to lower the experimental points or shift them towards lower K values. Thus any discrepancy between observation and calculation cannot be accounted for by such errors.

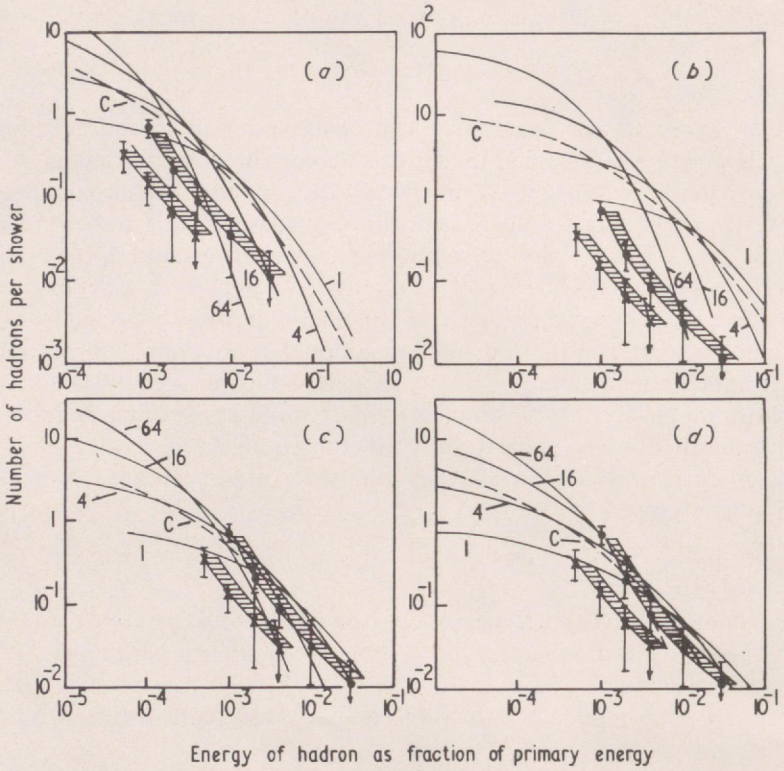

Figure 8. The fractional integral energy spectrum of high energy hadrons in EAS for the size groups less than $3{\cdot}2\times10^5$ (●) and greater than $3{\cdot}2\times10^5$ (×). The hadron energy is estimated as a fraction of the primary energy of the associated EAS. The experimental points are compared with the calculated integral energy spectra which are obtained for different values of elasticity (ϵ), interaction mean free path (λ) and atomic mass of primaries. Curves C represent a mixed composition approximating the one known at lower energies. The implications of such a comparison are discussed in a forthcoming paper. (*a*) $\lambda = 80\ \mathrm{g\,cm^{-2}}, \epsilon = 0{\cdot}5$; (*b*) $\lambda = 80\ \mathrm{g\,cm^{-2}}, \epsilon = 0{\cdot}6$; (*c*) $\lambda = 67\ \mathrm{g\,cm^{-2}}, \epsilon = 0{\cdot}5$; (*d*) $\lambda = 80\ \mathrm{g\,cm^{-2}}, \epsilon = 0{\cdot}4$.

2.7. The charge to neutral ratio of hadrons in EAS

The charge to neutral ratio (C/N) has been determined for different energies of hadrons at various distances from the core and for showers of different sizes. The procedure of acceptance of a hadron cascade for analysis is such that it is insensitive over a wide range to the actual value of the interaction mean free path of the hadron so that the detection efficiencies of charged and neutral events are nearly equal even if they have different interaction cross sections. The acceptance criteria for events to be identified as due to charged hadrons are: (i) the primary track must be identifiable as a single track in at least two compartments above the point of interaction; (ii) it must be uniquely identified from the detailed structure of the track in at least two views; (iii) the primary track direction must conform to the direction of the cascade axis within reasonable limits. To be identified as a neutral hadron the criteria adopted are: (i) the region above the point of interaction must be well within the illuminated and photographable region of the chamber; (ii) any track which could be mistaken as a likely charged primary in

one view, must be clearly eliminated as a stray track by reference to the other views. A final test before acceptance depends upon the answer to the following crucial question: 'Under exactly identical conditions, would the nature of the hadron be identified unambiguously if the primary was of the opposite type?' Many events which failed this test were rejected although they satisfied the other criteria. All the events were analysed twice. Twelve out of 874 events were found to be misidentified on re-analysis.

In table 3, the C/N ratios are given for three size and five energy groups. The figures in brackets correspond to weighted averages of the ratios in individual groups taking into account size variation and energy spectrum of hadrons. The unbracketed value is the ratio $\Sigma C/\Sigma N$. When hadrons of all energies greater than 25 GeV are combined, the ratio decreases from $6{\cdot}2 \pm 1{\cdot}3$ for sizes less than 3×10^5 to $3{\cdot}2 \pm 0{\cdot}5$ for sizes greater than 3×10^5 and then remains constant with increasing size. When combined for all sizes the ratio decreases with energy becoming $1{\cdot}1 \pm 0{\cdot}5$, for energies greater than 200 GeV where the geometric mean energy is about 300 GeV. In table 4, the ratios are given as a function of distance from the core for different energies but combined for all sizes. The energy estimate for the lowest energy group (10–25) GeV is inaccurate, and also possibly this energy group may be contaminated by recoil nucleons of energies less than 10 GeV, the extent of contamination depending upon distance from core and

Table 3. Charge to neutral ratio of hadrons in EAS—variation with shower size and hadron energy

Size \ Energy	10–25 GeV	25–50 GeV	50–100 GeV	100–200 GeV	> 200 GeV	For all energies > 25 GeV
$< 3{\cdot}2 \times 10^5$	18/7 $2{\cdot}6 \pm 1{\cdot}2$	52/3 17 ± 10	70/12 $5{\cdot}8 \pm 1{\cdot}8$	21/9 $2{\cdot}3 \pm 0{\cdot}9$	5/4 $1{\cdot}2 \pm 0{\cdot}8$	148/28 $5{\cdot}3 \pm 1{\cdot}1$ $(6{\cdot}2 \pm 1{\cdot}3)$
$3{\cdot}2 \times 10^5$ to $1{\cdot}8 \times 10^6$	77/8 $9{\cdot}6 \pm 3{\cdot}6$	138/44 $3{\cdot}1 \pm 0{\cdot}5$	146/46 $3{\cdot}2 \pm 0{\cdot}5$	39/24 $1{\cdot}6 \pm 0{\cdot}4$	5/4 $1{\cdot}2 \pm 0{\cdot}8$	328/118 $2{\cdot}8 \pm 0{\cdot}3$ $(3{\cdot}1 \pm 0{\cdot}5)$
$> 1{\cdot}8 \times 10^6$	55/13 $4{\cdot}2 \pm 1{\cdot}3$	112/29 $3{\cdot}9 \pm 0{\cdot}8$	66/25 $2{\cdot}6 \pm 0{\cdot}6$	16/6 $2{\cdot}7 \pm 1{\cdot}3$	0/1	194/61 $3{\cdot}2 \pm 0{\cdot}5$ $(3{\cdot}3 \pm 0{\cdot}5)$
For all sizes	150/28 $5{\cdot}4 \pm 1{\cdot}1$ $(5{\cdot}2 \pm 1{\cdot}7)$	302/76 $4{\cdot}0 \pm 0{\cdot}5$ $(3{\cdot}7 \pm 0{\cdot}7)$	282/83 $3{\cdot}4 \pm 0{\cdot}4$ $(2{\cdot}9 \pm 0{\cdot}4)$	76/39 $2{\cdot}0 \pm 0{\cdot}4$ $(2{\cdot}1 \pm 0{\cdot}4)$	10/9 $1{\cdot}1 \pm 0{\cdot}5$	670/207 $3{\cdot}2 \pm 0{\cdot}3$

Table 4. Charge to neutral ratio of hadrons in EAS—variation with distance from core

Distance \ Energy	10–25 GeV	25–50 GeV	50–100 GeV	100–200 GeV	10–200 GeV
< 8 m	72/8 $9{\cdot}0 \pm 3{\cdot}4$	169/42 $4{\cdot}0 \pm 0{\cdot}7$	194/58 $3{\cdot}4 \pm 0{\cdot}5$	61/27 $2{\cdot}3 \pm 0{\cdot}5$	496/135 $3{\cdot}7 \pm 0{\cdot}4$
> 8 m	78/20 $3{\cdot}9 \pm 1{\cdot}0$	133/34 $3{\cdot}9 \pm 0{\cdot}8$	88/25 $3{\cdot}5 \pm 0{\cdot}8$	15/12 $1{\cdot}3 \pm 0{\cdot}5$	314/91 $3{\cdot}5 \pm 0{\cdot}4$

shower size. For the energy group 100–200 GeV, the small decrease seen in the ratio at large distances could be a consequence of the difference in $\langle p_T \rangle$ or difference in the height of production of pions and nucleons. Due to the flatter lateral distribution of hadrons at lower energies the arbitrary value of 8 m used may not be large enough to separate pions and nucleons in the energy interval (25–100) GeV.

3. Comparison of results

The results reported in this paper on high energy hadrons may be summarized as follows:

(i) There is a tendency for the lateral distribution of high energy hadrons to flatten with increasing size.

(ii) The energy spectrum of hadrons in the energy range 50–800 GeV may be expressed by a power law of the form

$$N_n(>E) = BE^{-\gamma(N_e)}$$

where γ increases with N_e from a value of 1·4 at 5×10^4 to 2·2 at 4×10^5 or more, and remains at this high value up to 3×10^6 particles at 800 g cm^{-2}. The corresponding values of γ, if the maximum probable systematic errors are considered, are 1·2 and 1·9 respectively.

(iii) The variation of the number of hadrons $N_n(>E)$ as a function of shower size N_e may be expressed as

$$N_n(>E) = AN_e^{\alpha(E)}.$$

It is found that $\alpha(E)$ decreases with increasing E from a value of about 0·8 at $E > 50$ GeV to about 0·4 at $E > 400$ GeV.

(iv) The fractional hadron energy spectrum for hadrons of energy greater than 200 GeV is different for showers of size less than 3×10^5 and greater than 3×10^5 particles.

(v) There are cases of hadrons of energy greater than a few TeV appearing at distances up to 5·6 m from the core of showers.

(vi) The charge to neutral ratio of hadrons decreases with increasing energy of hadrons. In showers of size less than 3×10^5 the ratio has a value $6{\cdot}2\pm1{\cdot}3$ for hadrons of energy greater than 25 GeV and the value is $1{\cdot}2\pm0{\cdot}8$ for hadrons of energy greater than 200 GeV. For showers of size greater than 3×10^5 the corresponding values are $3{\cdot}2\pm0{\cdot}5$ and $1{\cdot}2\pm0{\cdot}8$.

We shall now examine to what extent some of these results are supported by observations of others.

The flattening of the lateral distribution of hadrons with increasing size of the shower has been reported in a number of earlier experiments (Chatterjee *et al* 1968a, Hasegawa *et al* 1965, Miyake *et al* 1969). It has also been observed by us in the data from the TAS which was operated as a second hadron detector in the present experiment. In fact the tendency for flattening is much more pronounced in the TAS results. However, as discussed earlier, for a variety of reasons the multiplate cloud chamber results are more reliable. The tendency for flattening is also seen in the cloud chamber experiment of Kameda *et al* (1965) at sea level.

In figure 9, we have compared the results on the variation of the number of hadrons of different energy as a function of size reported in the different experiments. It is seen that the results from the TAS in the present experiment, which are in essential agreement with the TAS results of Chatterjee *et al* (1968a), show that the absolute number of hadrons

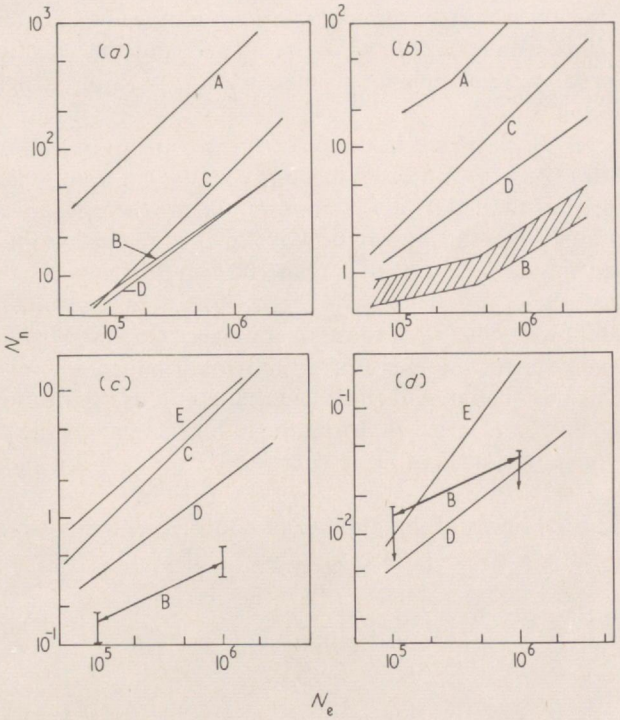

Figure 9. A comparison of the size variation of the number of hadrons with different energy thresholds obtained by various experimental groups using different hadron detectors. For clarity, statistical errors are not indicated in most of the results. (*a*) $E > 100$ GeV; (*b*) $E > 400$ GeV; (*c*) $E > 1$ TeV; (*d*) $E > 10$ TeV. In all four parts of the figure: curves A, present experiment (TAS); curves B, present experiment (Cl Ch); curves C, Kameda *et al* (1965); curves D, Miyake *et al* (1969); curves E, Matano *et al* (1969).

at energies greater than 100 and greater than 400 GeV are high compared to the cloud chamber results by more than an order of magnitude. We feel that the cloud chamber results on the flux and the spectrum of hadrons are more reliable than the TAS results for the following reasons. The cloud chamber has a much better spatial resolution and the energy of individual hadrons can be unambiguously determined by the method described by Vatcha *et al* (1972), even when multiple hadrons are incident which is generally the case with high energy hadrons close to the axis of shower. Also, the geometry in the cloud chamber experiment is well defined and only hadron interactions which occur well within the illumination region are considered for analysis. Since no visual detectors were used in conjunction with the TAS it was not possible to distinguish between the incidence of single high energy hadrons and multiple low energy hadrons and γ rays which can deposit an equal amount of energy. The abundance of such events is clearly revealed by the analysis of cloud chamber photographs obtained in the present experiment. The TAS, which is a more reliable instrument for measurement of energy when a single hadron is incident, thus reduces to an instrument for measuring the energy flow in hadrons and γ rays at short distances from the core. Also, because of leakage from the sides it becomes difficult to define precisely the aperture of the instrument. It may be pointed out that the results presented earlier on the time structure of hadrons using the TAS (Tonwar *et al* 1971) are not affected by these considerations, since in the

timing experiment mostly isolated events of energy about a few tens of GeV arriving up to distances of 20 m from the core were considered and the selection system was such that if the hadrons were associated even with a few prompt particles on the TAS, the events were rejected.

At a shower size of 10^5 particles, in the present experiment, in that of Miyake *et al* (1969) at Mt Norikura (2·8 km) and of Kameda *et al* (1965) at sea level, the number of hadrons of energy greater than 100 GeV is about 7. While there is agreement between the results of the present experiment and of Miyake *et al* regarding the size variation of the number of hadrons of energy greater than 100 GeV, the experiments of Kameda *et al* give a much faster rise. For hadrons of higher energy our results with the cloud chamber give a much lower value than those of Kameda *et al* and Miyake *et al*. In our experiment, as already stated, the energies of individual hadrons even at the highest energies are determined by the integral track length method using Monte Carlo simulations for calibration (Vatcha *et al* 1972). From the published papers the precise method adopted by others for the determination of energy of hadrons in the cloud chamber is not clear.

Our results on the variation of the number of hadrons with associated size N_e and energy of hadron E may be parametrized as follows:

$$N_n(>E, N_e) = 7{\cdot}3\left(\frac{N_e}{10^5}\right)^{0{\cdot}71}\left(\frac{E}{100}\right)^{\gamma} \qquad \text{for } (50 < E < 800)\ \text{GeV}$$

where

$$\gamma = \ln\left(\frac{N_e}{N_o}\right)^{-\alpha} \qquad \text{for } 5\times10^4 < N_e < 4\times10^5$$

and

$$\gamma = -\beta \qquad \text{for } 4\times10^5 < N_e < 3\times10^6$$

where

$$N_o = 1{\cdot}4\times10^3; \qquad \alpha = 0{\cdot}41, \qquad \beta = 2{\cdot}32.$$

For a maximum systematic underestimate of hadron energies by about 50%, N_o, α, β may be altered to

$$N_o = 1{\cdot}35\times10^3; \qquad \alpha = 0{\cdot}33, \qquad \beta = 1{\cdot}88.$$

The break in the N_n against N_e curve at $N_e = (3\text{–}4)\times10^5$ for high energy hadrons is not very significant statistically in our experiment; however, similar effects have been observed for low energy hadrons (few GeV) by Chatterjee (1964) and Danilova *et al* (1964) and also for low energy muons ($\sim$ 1 GeV) by Chatterjee *et al* (1968b). The results of Kameda *et al* on high energy hadrons do not show a break in the N_n against N_e curve. Their observations are at sea level and for showers of size greater than 10^5 particles. In our experiment the indication of a break is at about 3×10^5 particles at 800 g cm^{-2}. Since the break should ultimately be connected with the energy per nucleon of the primary particle, the break at 3×10^5 at 800 g cm^{-2} could occur at say about 10^5 at sea level. Since the observations of Kameda *et al* do not extend below 10^5, they cannot confirm or negate the evidence for a break. In most of the earlier experiments with non-visual detectors the slope of the integral hadron energy spectrum over a wide band of energies was found to be about 1·0 independent of shower size. The experiments of Miyake *et al* at 2·8 km showed a steepening of the spectrum, the slope changing to

about 1·8, beyond 500 GeV. The results of Matano *et al* (1969) at sea level have shown that at energies greater than 1·7 TeV, the slope changes to about 2·1. In our results the steepening is apparent even at lower energies.

The tendency for the charge to neutral ratio for hadrons to decrease with increasing energy is seen in the results of Kameda *et al* also. However, the results differ in absolute values. The ratios given by Kameda *et al* for all sizes are

$6{\cdot}0 \pm 1{\cdot}0$ for $E < 500$ GeV;

$2{\cdot}5^{+1{\cdot}5}_{-0{\cdot}5}$ for $E > 500$ GeV;

and

$1{\cdot}5 \pm 0{\cdot}5$ for $E > 1000$ GeV.

In our experiment, the ratio decreases to $1{\cdot}1 \pm 0{\cdot}5$ at $E > 200$ GeV. As already pointed out in connection with the discrepancy in the absolute number of hadrons, differences in the estimation of energy of hadrons in the two experiments may explain to some extent the discrepancies in the absolute values of C/N ratios also.

The evidence for a change in the value of C/N ratio for high energy hadrons as a function of shower size and distance from core and a distinct difference in the fractional hadron energy spectra for showers of size less than and greater than 3×10^5 particles and the steepening of the hadron spectra with size are important features that have been revealed by the present experiment which have not been reported by other investigators.

The implications of these various results on high energy hadrons in air showers from the point of view of the primary composition and strong interaction characteristics at ultra-high energies are discussed in the following papers.

Acknowledgments

We wish to thank Dr B K Chatterjee for collaboration in the early stages of the experiment. It is a pleasure to acknowledge the profitable discussions with Professor S Naranan, Drs G T Murthy, M V Srinivasa Rao, K Sivaprasad and S C Tonwar at various stages. Sri N V Gopalakrishnan carried out the tedious job of analysing several thousands of cloud chamber photographs. Technical services were provided by Sri A R Apte and Sri S G Khairatkar.

References

Chatterjee B K 1964 *PhD Thesis* University of Bombay

Chatterjee B K *et al* 1968a *Can. J. Phys.* **46** S136–41

—— 1968b *Can. J. Phys.* **46** S131–5

Danilova T V, Denisov E V and Nikolsky S I 1964 *Sov. Phys.–JETP* **19** 1056–66

Feynman R P 1969 *Phys. Rev. Lett.* **23** 1415–7

Hasegawa H, Noma M, Suga K and Toyoda Y 1965 *Proc. 9th Int. Conf. on Cosmic Rays, London* vol 2 (London: The Institute of Physics and The Physical Society) pp 642–5

Kameda T, Maeda T, Oda H and Sugihara T 1965 *Proc. 9th Int. Conf. on Cosmic Rays, London* vol 2 (London: The Institute of Physics and The Physical Society) pp 681–4

Matano T, Machida M and Ohta K 1969 *Proc. 11th Int. Conf. on Cosmic Rays, Budapest* vol 3 (Budapest: Central Research Institute for Physics) pp 451–62
Miyake S *et al* 1969 *Proc. 11th Int. Conf. on Cosmic Rays, Budapest* vol 3 (Budapest: Central Research Institute for Physics) pp 463–9
Murthy G T 1967 *PhD Thesis* University of Bombay
Ramana Murthy P V, Sreekantan B V, Subramanian A and Verma S D 1963 *Nucl. Instrum. Meth.* **23** 245–54
Tonwar S C and Sreekantan B V 1971 *J. Phys.* A: *Gen. Phys.* **4** 868–82
Vatcha R H 1972 *PhD Thesis* University of Bombay
Vatcha R H, Sreekantan B V and Tonwar S C 1972 *J. Phys.* A: *Gen. Phys.* **5** 859–76

J. Phys. A: Math., Nucl. Gen., Vol. 6, July 1973. Printed in Great Britain.

Evidence for change in the characteristics of strong interactions at ultra-high energies

R H Vatcha and B V Sreekantan

Tata Institute of Fundamental Research, Bombay-5, India

Received 7 December 1972

Abstract. In this paper an attempt has been made to understand the experimental results on the size dependence of several properties of high energy hadrons reported in a previous paper in terms of the characteristics of high energy collisions and primary composition using detailed Monte Carlo simulations. It is shown that the behaviour of the high energy hadron component, especially the size dependence, cannot be accounted for in terms of a change of primary composition alone in the energy range 10^{14}–10^{16} eV which has been suggested by some of the earlier investigations to explain certain properties of air showers. The present analysis strongly suggests the need for invoking rather drastic changes in the characteristics of strong interactions, at ultra-high energies. The details about the trends in the changes will be discussed in a subsequent paper.

1. Introduction

In the preceding paper (Vatcha and Sreekantan 1973, to be referred to as I) we have presented experimental results on changes in the properties of hadrons of energy greater than 25 GeV in air showers of size 5×10^4 to 3×10^6 particles at 800 g cm^{-2}, obtained by operating a 2 m^2 multiplate cloud chamber at the centre of the TIFR air shower array at Ooty and have compared the results with those of other experiments. In this paper we make a comparison of the experimental results with expectations based on existing Monte Carlo simulations of air showers in which the parameters of high energy collisions are adopted as reasonable extrapolations of measurements and trends at machine energies ($\leqslant 70$ GeV). The properties of heavy primary showers are obtained by a simple superposition of proton showers of the requisite number and energy per nucleon. The comparison shows a wide disparity between the experimental and calculated results. We find it difficult to explain in a consistent manner the size dependence of the properties of hadrons by any type of change in primary composition in the relevant energy range 10^{14}–10^{16} eV. While the variation with shower size of some of the properties of the high energy hadrons demands a drastic transformation of the primary composition from a lighter to a heavier component within this energy range, certain other properties require just the opposite trend, suggesting thereby that the discrepancies cannot be removed by composition change alone. Besides there are several properties of hadrons which clearly show that the parameters of strong interactions like inelasticity and/or interaction mean free path and composition of secondary particles at ultra-high energies have to be necessarily different from those determined at machine energies.

2. Comparison of experimental results with Monte Carlo simulations

In recent years a number of investigators have carried out Monte Carlo simulations of the different components of air showers. We have chosen to compare our experimental results with the calculations of Murthy *et al* (1968) since in these calculations the results on the various parameters of interest are available for the specific altitude at which the present experiment has been carried out, that is 800 g cm^{-2}, and also in a form suitable for direct comparison. Most of the later simulations (see, for example, Greider 1970 and references therein) agree well with the calculations of Murthy *et al.*

In table 1, the details of the eight models, on the basis of which the hadronic cascades have been simulated by Murthy *et al*, are given. It is seen that Murthy *et al* have considered three different laws of multiplicity, the formation of isobars and also the formation of nucleon–antinucleon pairs. The simulations have been carried out both for proton and heavy primary induced showers.

In table 2, the experimental results on the variation of the slope of the hadron spectrum in the energy range 50–800 GeV with shower size is compared with the calculated slopes of Murthy *et al.* According to the experiment, the slope changes from about 1·3 or more at about 10^5 to approximately 1·9 or more at about 4×10^5 and thereafter remains constant. The calculated value however is 1·2 for proton and iron showers at all sizes and for all the models except the HLN model in which the value is 1·5. It is important to note that the calculations do not give any change of slope with size.

In table 3, the absolute number of hadrons of energy greater than 100 GeV in showers of different sizes obtained in the Ooty experiment are compared with the calculated values for both proton and iron induced showers. It is seen that the observed numbers are less by a factor of four to ten if we consider proton showers and models in which $N\bar{N}$ production is not considered. The disparity is enhanced by a further factor of two if $N\bar{N}$ production is considered which, as we shall see, is quite essential to explain various results. There is evidence for increase in the cross section for the production of $N\bar{N}$'s in the time structure experiments of Tonwar and Sreekantan (1971) and also in the ISR experiments (Bertin *et al* 1972). The disparity is higher still if we consider the showers to be due to all heavy primaries like iron.

In table 4, the experimental values on the charge to neutral ratio (C/N) of hadrons for two different size groups (ie $< 3 \times 10^5$ and $\geqslant 3 \times 10^5$ particles) have been compared with the calculated values for proton showers of size of the order of 3×10^5 particles. It is seen that unless $N\bar{N}$ production is considered, the disparity between the experimental and calculated values is by more than a factor of twenty. We shall consider in detail later in § 4 how the presence of heavy primaries will influence the C/N ratio.

Greider (1971) has recently carried out quite extensive Monte Carlo simulations of air showers and has considered different types of isobar and fireball production, and also $N\bar{N}$ production, and distribution of transverse and longitudinal momenta of secondaries. The results, however, are not directly available for our altitude of 2·2 km and shower sizes are not calculated, and therefore direct comparison with experimental results presents some difficulty. However, by a reasonable interpolation we have compared our results with his calculations. In Greider's calculations except in some extreme models, in general the slope of the integral energy spectrum in the range 25–800 GeV is less than 1·5. The absolute number of high energy hadrons ($\gtrsim 100$ GeV) in most of his models is higher than what is experimentally observed. The C/N ratio in all his models has a value greater than ten at a few hundred GeV and the ratio increases

Table 1. Details of models used by Murthy *et al* for simulation of hadron cascades

	Model QLN		Model LLN		Model HLN		Model IBN		
							Nucleon		
	Nucleon	Pion	Nucleon	Pion	Nucleon	Pion	Fireball	Isobar	Pion
Multiplicity, M	$2{\cdot}7\,E^{1/4}$		$5{\cdot}26\ln(E/18+1)$		$0{\cdot}96\,E^{1/2}$		$0{\cdot}25\,E^{1/2}$	3	$0{\cdot}96\,E^{1/2}$
Inelasticity, K	0·5	1	0·5	1	0·5	1	0·2	distribution with average 0·3	1
Mean free path in g cm^{-2} air	80	120	80	120	80	120	80		120
Fraction of $N\bar{N}$ produced, f	$7(500/E+1)^{-1}$		$7(500/E+1)^{-1}$		$7(500/E+1)^{-1}$		isobar excitation probability is 0·7		
Energy spectrum of created particles	exponential		exponential		exponential		$7(500/E+1)^{-1}$ distribution decided by kinematics		$7(500/E+1)^{-1}$ exponential

E is the projectile energy.

The average energy of created pions and nucleons is assumed to be proportional to their respective masses.

QL, LL, HL, and IB models are identical with QLN, LLN, HLN, and IBN models, respectively, except that all the created particles are assumed to be pions, ie $f = 0$. QL, LL, and HL stand for 'quarter law', 'log law' and 'half-law' of multiplicity variation.

Table 2. Slope of the hadron spectrum 50–800 GeV at 800 g cm^{-2}

		Calculated			
		Proton primaries		Iron primaries	
Shower size	Observed	QLN, LLN, IBN	HLN	QLN, LLN, IBN	HLN
10^5	1·2†–1·4	1·2	1·5	1·2	1·5
4×10^5	1·9†–2·3	1·2	1·5	1·2	1·5
10^6	1·9–2·3	1·2	1·5	1·2	1·5
3×10^6	1·9–2·3	1·2	1·5	1·2	1·5

† The values 1·2 and 1·9 correspond to the values of the slope when the maximum probable systematic underestimate of energy is taken into account.

Table 3. Variation of the number of hadrons ($\geqslant 100$ GeV) with shower size

	Observed number of hadrons of $E \geqslant 100$ GeV per shower	Calculated			
		Proton primaries		Iron primaries	
Shower size		Without N$\bar{\text{N}}$	With N$\bar{\text{N}}$	Without N$\bar{\text{N}}$	With N$\bar{\text{N}}$
10^5	7·3	30	85		
4×10^5	20	120	320		
10^6	37	300	800	550	1200
3×10^6	82	800	2000		

Table 4. Charge to neutral ratio of hadrons

Energy (GeV)	Observed shower size at 800 g cm^{-2}		Calculated	
	$< 3 \times 10^5$	$\geqslant 3 \times 10^5$	Without N$\bar{\text{N}}$	With N$\bar{\text{N}}$
25	$6{\cdot}2 \pm 1{\cdot}3$	$3{\cdot}0 \pm 0{\cdot}3$	200	2–4
50	$3{\cdot}8 \pm 0{\cdot}9$	$2{\cdot}6 \pm 0{\cdot}3$	130	1·5–3
100	$1{\cdot}9 \pm 0{\cdot}6$	$1{\cdot}8 \pm 0{\cdot}4$	65	1·2–2·2
200	$1{\cdot}2 \pm 0{\cdot}8$	$1{\cdot}2 \pm 0{\cdot}8$	25	1·1–1·9

with hadron energy which is opposite to the trend seen in the present experiment. Also, in none of the models is there a trend for the energy spectrum to steepen with increasing primary energy.

Thus we come to the conclusion that the experimental results on the variation of slope of the hadron spectrum, the absolute number and charge to neutral ratio of hadrons as a function of hadron energy and shower size are not in conformity with the various Monte Carlo simulations. This suggests that either the collision characteristics at ultra-high energies are considerably different from the extrapolations from machine

energies, or the primary composition is radically changing in the energy range 10^{14}–10^{16} eV, or both causes are operative. We shall now examine which of these possibilities is indicated by the properties of high energy hadrons, especially their size dependence.

3. Variation of the number of hadrons with size

The results on the variation of the number of hadrons with shower size have shown that the slope of the N_n against N_e curve flattens with increasing hadron energy. For hadrons of higher energy this flattening could even be due to a radical change of slope of the curve from a low to a high value within the shower size investigated (ie 5×10^4–5×10^6 particles at 800 g cm^{-2}). Several experiments on the variation of the number of low energy hadrons (few GeV) and of low energy muons (few GeV) with shower size have clearly shown the existence of a change of slope in this size range. The early results of Nikolsky (1956) on this change of slope were interpreted by Peters (1960) on the basis of a model of changing primary composition, which he attributed to a rigidity cut-off in the galactic magnetic field. Later, Chatterjee (1964) explained a variety of results in EAS on the basis of such a model. The behaviour of the high energy γ ray spectrum in the atmosphere (Yash Pal and Tandon 1966) and the slow increase of high energy muons with shower size (Sivaprasad 1972) also lend support to the hypothesis of a changing primary composition in the energy range 10^{14}–10^{16} eV.

Let us examine in a qualitative manner what should be the trend in the change of the average mass of the primary, if the change of slope is to be attributed to change of composition. Let $N_n(P)$ be the number of hadrons of energy greater than E in showers initiated by protons; $N_n(A)$ the number of hadrons of energy greater than E in showers initiated by heavy primaries of atomic mass A. Assume $N_n(P) \sim N_e^{\alpha}$ for *all* sizes, then $N_n(A) \sim N_e^{\alpha} A^{1-\alpha}$. Thus the slope of the N_n–N_e curve of a heavy primary A (as also mixed composition which does not change with size) is the same as that of a proton primary. Suppose the composition undergoes a change in a size interval $N_{e(1)}$–$N_{e(2)}$. Assume that the variation of the mean atomic mass $\langle A \rangle$ in this size interval is expressed by

$$\langle A \rangle \sim N_e^q,$$

then†

$$N_n(A) \sim N_e^{\alpha+q-\alpha q}.$$

Depending upon the values of α and q, there are four possible behaviours of a change in the slope of the N_n against N_e curve in the size interval $N_{e(1)}$–$N_{e(2)}$. These possibilities are illustrated in figure 1.

If the size $N_{e(2)}$ is identified with the value of the order of 3×10^5 as is expected from other results, it is clear that in order to explain the break the appropriate parameters are either $\alpha < 1$, $q < 0$ or $\alpha > 1$, $q > 0$. The second possibility is unlikely as α is less than 1 in the present experiment for high energy hadrons as well as in the other experimental results on the size variation of low energy hadrons and muons. Since this implies that $q < 0$, a *changing composition which becomes progressively lighter with*

† Actually the N_n–N_e curve for a mixed composition is given by $N_n(\langle A \rangle) \sim N_e^{\alpha} \Sigma W_i A_i^{1-\alpha}$ subject to $\Sigma W_i = 1$ and $\langle A \rangle = \Sigma W_i A_i$ where the fraction of primaries of atomic mass A_i out of all primaries is W_i. To explain the effects quantitatively the actual mixed composition is replaced by $\langle A \rangle$ which is not strictly correct. The conclusions, however, are not affected by such a procedure.

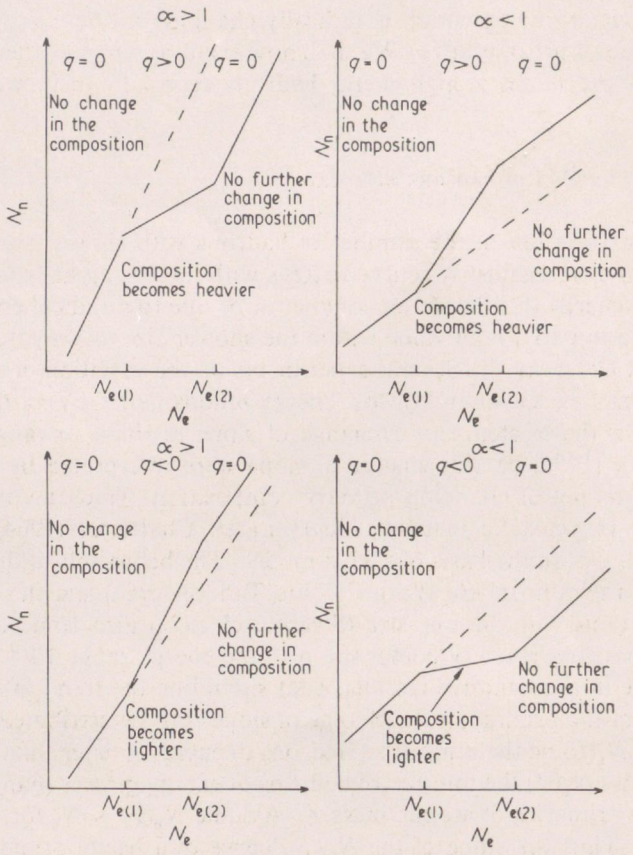

Figure 1. Sketches illustrating the behaviour of the N_n against N_e curve when the primary composition changes corresponding to the size interval $N_{e(1)}$ to $N_{e(2)}$ for different ranges of values of α and q.

increasing size is required to explain the observed changes in slope. An anomalous feature is the absence of a change of slope in the intermediate energy range of 25–100 GeV in the experimental results.

4. Charged to neutral ratio of hadrons

The ratio of charged to neutral hadrons in an EAS may be written as

$$R(E_0) = \frac{n_{\pi^\pm}(E_0)+n_{K^\pm}(E_0)+\frac{1}{2}n_{N\bar{N}}(E_0)+\frac{1}{2}}{\frac{1}{2}n_{N\bar{N}}(E_0)+n_{K^0\bar{K}^0}(E_0)+\frac{1}{2}} \tag{1}$$

where n_X is the number of hadrons of type X at the observation level produced in an EAS initiated by a nucleon of energy E_0. Equation (1) is valid even if the charge exchange probability in nucleon interactions is small ($\lesssim 20\%$) since, on the average, the survivor undergoes a number of interactions so that whatever be the nature of the primary nucleon the probability of the survivor being a proton is $\frac{1}{2}$.

If no $N\bar{N}$ or kaon production is considered then

$$R(E_0) = 2n_{\pi^{\pm}}(E_0)+1 \tag{2}$$

which increases with E_0 or size.

In the case of a shower initiated by a heavy primary of total energy E_0 and mass number A, the charge to neutral ratio is a function of energy per nucleon and not total energy, that is,

$$R(E_0)_{\text{heavy primary}} = R\left(\frac{E_0}{A}\right)_{\text{nucleon}}.$$

The experimental results indicate a decrease in the ratio with increasing size and to explain this on the basis of a change in primary composition *E_0/A must decrease with increasing E_0*. Thus the mechanism of enriching heavy primaries with increasing energy must be faster than that expected from a model invoking magnetic rigidity cut-off in which the average energy per nucleon does not decrease with increasing energy.

Assuming $n_{K^{\pm}} = n_{K^0\bar{K}^0}$, the fraction of nucleons and kaons among the hadrons is

$$f_{NK} = \frac{2}{R(E_0)+1}.$$

At a shower size of 3×10^6, $R = 3{\cdot}2$ so that $f_{NK} = 0{\cdot}476$. Since the total number of hadrons of energy greater than 25 GeV at size 3×10^6 is 1000, the number of nucleons and kaons is 476. Even if we assume that the showers are all due to iron nuclei the maximum contribution from survivors is 56 nucleons so that at least 420 $N\bar{N}$ pairs and kaons must be secondaries. Thus a change in composition alone cannot explain the C/N ratio at large sizes. The results on the time structure of hadrons in EAS (Tonwar and Sreekantan 1971) can be interpreted only in terms of an increase in $N\bar{N}$ production and cannot be explained by an increase in kaon production.

If the decrease in R at a shower size greater than 3×10^5 particles is to be attributed to a further increase in $N\bar{N}$ production it is obvious that the excess nucleons must arise from interactions of energies of 10^6 GeV or more near the top of the atmosphere.

5. Variation of the slope of the hadron spectrum

The slope of the integral hadron energy spectrum is obviously a function of energy per nucleon and not of total energy of the primary. Consequently in a simple superposition model the energy spectrum of high energy hadrons in a shower due to a heavy primary will be steeper than in a proton shower of the same primary energy. The experimental data show a steepening of the slope of the hadron spectrum with increase of shower size up to a size value of the order of 4×10^5. If this feature has to be explained by change of primary composition, then the transformation to heavy primaries must occur very fast so that the energy per nucleon of the primary is brought down rapidly. It may be pointed out that in a rigidity cut-off model while the primary composition is changing the average energy per nucleon does not decrease, and therefore we should not expect a steepening of slope with increasing size.

It is possible that due to the onset of collective interactions at high energies in the collisions of heavy primaries the spectrum of high energy hadrons in heavy primary showers may be considerably different from what is expected on the basis of a simple superposition model. It may be mentioned however that Orford and Turver (1969) have considered the effects of coherent interactions of heavy primaries in connection with their calculations on the behaviour of the high energy muon component and have come to the conclusion that collective interactions are of little significance as far as high energy muons are concerned.

6. Tendency for flattening of the hadron lateral distribution

As discussed in paper I (Vatcha and Sreekantan 1973), the cloud chamber results also show a tendency for the lateral distribution of high energy hadrons to flatten with increasing size, though it is not so pronounced as in the experiments with non-visual detectors. The Monte Carlo simulations indicate if at all an opposite trend—the distribution is slightly flatter in small size showers. The lateral distribution of hadrons is a function of the energy per nucleon and not the total energy of the primary. If a change in the primary composition is responsible for the flattening, then it is evident that the energy per nucleon has to be reduced rapidly with increasing size, which means that the primary composition must become rapidly heavier. The Monte Carlo simulations of Greider (1970) show that in some models an increase in the average height of first interaction of the primary tends to flatten the lateral distribution of hadrons. As the primaries become heavier the average height of primary collision increases and would thus serve as an additional cause for flattening as the primary composition becomes heavier. The mechanism of fragmentation of heavy nuclei plays an important role in the determination of the lateral distribution of hadrons. For example, if the heavy nucleus fragments in such a way that only one nucleon interacts at a time, then the effective height of the cascade maximum is lowered much more than in the case of a single act of fragmentation. Thus the amount of flattening would depend on the exact mechanism of fragmentation. What is clear is that a change from a lighter to a heavier component is necessary for the flattening to occur with increasing size.

7. The fractional hadron energy spectrum

In figure 2 we have reproduced the fractional hadron energy spectrum given in figure 8 of the previous paper, wherein the observed integral hadron energy spectrum is plotted as a fraction of the primary energy of the associated shower after classifying the data into two broad groups $N_e < 3 \times 10^5$ and $N_e \geqslant 3 \times 10^5$. In general, these hadrons at the observational level are a mixture of the survivors of the incident primaries and of secondaries produced in various collisions. In figure 2 the different curves correspond to the spectra of the surviving primaries calculated for primaries of mass numbers 1, 4, 16 and 64 (chosen for convenience) and on the basis of certain pairs of values of elasticity and interaction mean free path. The broken curve 'C' represents a mixed composition approximating the one known at lower energies. The calculated spectra† are obtained from the fluctuations in the number of interactions of the primary before reaching the level of observation.

† These curves were obtained by Dr B K Chatterjee.

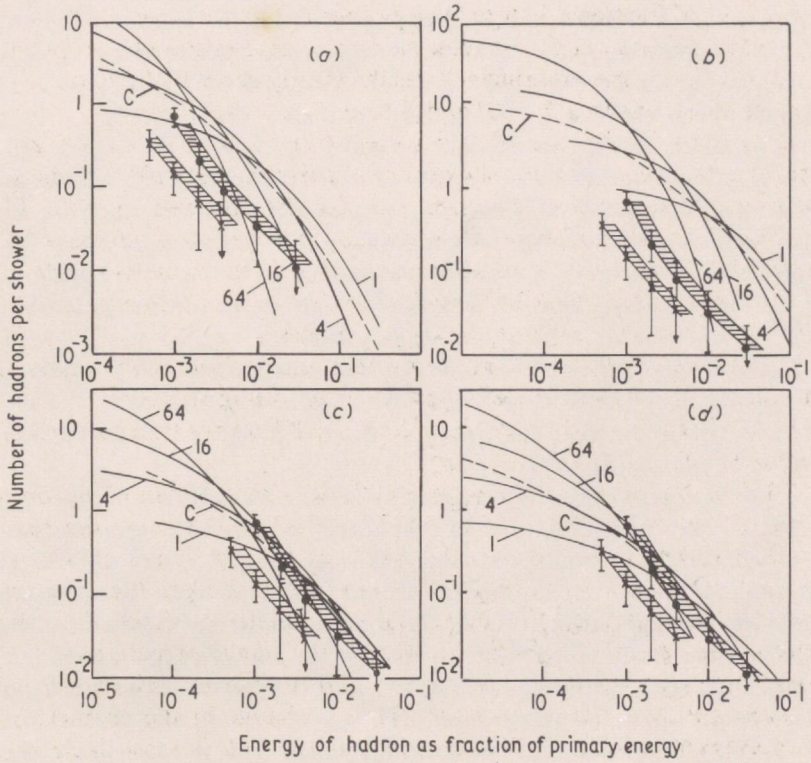

Figure 2. The fractional integral energy spectrum of hadrons of energy greater than 200 GeV for the size groups less than $3{\cdot}2 \times 10^5$ (●) and greater than $3{\cdot}2 \times 10^5$ (‡) at Ooty. The hadron energy is expressed as a fraction of the primary energy of the associated EAS. The experimental points are compared with calculated integral energy spectra for different pairs of values of interaction mean free path λ and elasticity ϵ. The different curves in each figure correspond to different mass numbers (1, 4, 16, 64) of primaries. The dashed curve C corresponds to a mixed composition. (*a*) $\lambda = 80\ \mathrm{g\,cm^{-2}}$, $\epsilon = 0{\cdot}5$; (*b*) $\lambda = 80\ \mathrm{g\,cm^{-2}}$, $\epsilon = 0{\cdot}6$; (*c*) $\lambda = 67\ \mathrm{g\,cm^{-2}}$, $\epsilon = 0{\cdot}5$; (*d*) $\lambda = 80\ \mathrm{g\,cm^{-2}}$, $\epsilon = 0{\cdot}4$.

For a primary of atomic mass 'A' the number of nucleon survivors at the level of observation with a fractional energy greater than K is given by

$$N_n(>K) = A \sum_{l=0}^{R} \frac{e^{-X} X^l}{l!} \qquad \text{with} \qquad K = \frac{\epsilon^R}{A},$$

where $X = 800/\lambda$, $800\ \mathrm{g\,cm^{-2}}$ being the atmospheric depth corresponding to Ooty, λ = interaction mean free path, and ϵ = elasticity in nucleon–air nucleus collisions. Since the spectrum of the survivors of primaries of a given A is determined only by the value of λ and ϵ for any given depth X, and if λ, ϵ and A do not change with energy, then the spectrum should remain the same for all sizes. If the comparison between calculation and observation is to be meaningful, survivors must be well separated from secondaries so that secondaries should be negligible in the energy region considered here.

If we consider the survivor spectra for $\lambda = 80\ \mathrm{g\,cm^{-2}}$ and $\epsilon = 0{\cdot}5$, which are the normally accepted values at lower energies, then the observed spectra are well below the expected survivor spectra for protons as well as for heavier primaries, and there is no scope for any contribution from secondaries at all. The disagreement is more serious

in the case of fractional hadron energy spectra for the large size ($> 3 \times 10^5$) showers. As already pointed out there should be no size dependence of this spectrum for fixed λ, ϵ and A whereas the experimental results clearly show a difference in the spectra for showers of size less than 3×10^5 and greater than 3×10^5.

If we consider the pair of values $\epsilon = 0{\cdot}4$ and $\lambda = 80$ or $\epsilon = 0{\cdot}5$ and $\lambda = 68$, then there is better agreement for showers of size less than 3×10^5, but the same values do not give a spectrum that is compatible with the observed spectrum for larger sizes. It is also clear that a change in composition at a size value of about 3×10^5 does not resolve the discrepancy. A more drastic change in the value of ϵ and/or λ is necessary for the larger sizes. Therefore one feature that seems to emerge is that the values of ϵ and/or λ are not the same at ultra-high energies.

It must be emphasized that the comparisons indicate only trends and the actual discrepancy is expected to be larger for the following reasons:

(i) Statistical errors in the energy estimate of hadrons tend to increase the observed number of hadrons at any energy.

(ii) Size to primary energy conversion is done on the basis of proton primaries only so that E_0 may be underestimated and hence 'K' may be overestimated.

(iii) Secondaries would contribute at least for low values of 'K'. Thus normally the contamination from secondaries would tend to steepen the spectrum of survivors unless the energy spectrum of secondaries is similar to those of survivors. Possible sources of underestimating either the flux or the energy of hadrons in the experimental results have been considered in paper I and it appears unlikely that any systematic biases could affect the conclusions. Thus a change in the characteristics of strong interactions from a few TeV to several hundred TeV is most likely and a change in primary composition alone cannot explain the above results.

The present results agree qualitatively with those of Grigorov *et al* (1965), who have concluded that at sizes of 10^5 particles or more at about 3·2 km above sea level, the concept of a leading particle propagating the air shower should probably be abolished.

8. Conclusions

The steepening of the hadron spectrum, the variation of the C/N ratio, the tendency for flattening of the lateral distribution with increasing size, all suggest that if the size dependence is due to a change of primary composition, then the composition should change rather suddenly from a lighter to a heavier component with increasing primary energy from 10^{14} to 10^{16} eV. On the other hand, the variation of the number of low and high energy hadrons and muons requires a change of primary composition from a heavier to a lighter component with increasing primary energy. To explain the variation of the average steepness parameter of electrons with size as well as to understand the correlations between the structure functions of hadronic, muonic and electronic components observed at Ooty, Chatterjee (1964) suggested a model in which the primary composition becomes increasingly lighter as the size increases. Thompson *et al* (1969) have shown that several results on the muonic component of EAS either require no change in primary composition or a change of composition which becomes progressively lighter with increasing primary energy at energies around 10^{15} eV.

Thus the hypothesis of changing primary composition leads to serious contradictions. Moreover, the rather low value of C/N ratio for large size showers where the absolute number of hadrons is quite high indicates the need for copious production of nucleon–

antinucleon pairs. The further decrease in the C/N ratio at higher shower sizes implies a further increase in the production of $N\bar{N}$'s, which has to necessarily take place only at energies of 10^{15} eV or more. The distinct difference in the fractional hadron energy spectra for different size groups and the observation that the experimental spectra fall below those expected for survivors on the basis of normally accepted values of inelasticity and interaction mean free paths, suggest that these parameters also need revision at higher energies.

In a subsequent paper we present trends of ultra-high energy interactions suggested by the change in the properties of high energy hadrons in air showers and discuss to what extent such trends succeed in explaining some of the important properties of air showers.

References

Chatterjee B K 1964 *PhD Thesis* University of Bombay

Bertin A *et al* 1972 *Phys. Lett.* **38B** 260–4

Greider P K F 1970 *Institute for Nuclear Study Report No* J125

—— 1971 *Proc. 12th Int. Conf. on Cosmic Rays, Hobart* 1971 vol 3 (Hobart: University of Tasmania) pp 970–81

Grigorov N L *et al* 1965 *Proc. 9th Int. Conf. on Cosmic Rays, London* 1965 vol 2 (London: The Institute of Physics and The Physical Society) pp 649–50

Murthy G T *et al* 1968 *Can. J. Phys.* **3** S147–63

Nikolsky S I 1956 *Proc. Conf. on Extensive Air Showers, Oxford* pp 16–20

Orford K J and Turver K E 1969 *Proc. 11th Int. Conf. on Cosmic Rays, Budapest* 1969 vol 3 (Budapest: Central Research Institute for Physics) pp 585–91

Peters B 1960 *Proc. Int. Conf. on Cosmic Rays, Moscow* 1959 vol 3 (Moscow: Viniti) pp 157–66

Sivaprasad K 1972 *PhD Thesis* University of Bombay

Thompson M G, Turner M J L, Wolfendale A W and Wdowczyk J 1969 *Proc. 11th Int. Conf. on Cosmic Rays. Budapest* 1969 vol 3 (Budapest: Central Research Institute for Physics) pp 615–20

Tonwar S C and Sreekantan B V 1971 *Proc. 12th Int. Conf. on Cosmic Rays, Hobart* 1971 vol 3 (Hobart: University of Tasmania) pp 177–80

Vatcha R H and Sreekantan B V 1973 *J. Phys.* A: *Math., Nucl. Gen.* **6** 1050–66

Yash Pal and Tandon S N 1966 *Phys. Rev.* **151** 1071–5

J. Phys. A: Math., Nucl. Gen., Vol. 6, July 1973. Printed in Great Britain.

Trends in the energy dependence of strong interaction characteristics at ultra-high energies

R H Vatcha and B V Sreekantan
Tata Institute of Fundamental Research, Bombay-5, India

Received 7 December 1972

Abstract. The trends in the energy dependence of strong interaction characteristics that reveal themselves when an attempt is made to bring about a closer agreement between experimentally observed size dependence of several properties of high energy hadrons in air showers and the corresponding Monte Carlo simulations, are discussed. The discussion shows the need for an increase in the inelasticity and interaction cross section of both pions and nucleons at ultra-high energies, as also an increase in the cross section for the production of nucleon–antinucleon pairs and also the need for postulating a process similar to the gammaization process of Nikolsky according to which a considerable fraction of energy is transferred to the soft component by-passing the normal pionization.

1. Introduction

In two earlier papers (Vatcha and Sreekantan 1973a, b, to be referred to as I, II) we have presented experimental results on the high energy hadron component of extensive air showers and from a comparison of the results with expectations based on Monte Carlo simulations have come to the conclusion that several properties of air showers cannot be explained in a consistent manner within the framework of the characteristics of ultra-high energy interactions extrapolated from low energies. We have also shown that a change of primary composition alone in the energy range 10^{14}–10^{16} eV is unable to explain the observations and that certain drastic changes are essential in strong interaction characteristics at ultra-high energies. In particular, we have demonstrated from the behaviour of the charge to neutral ratio of hadrons at high energies, that there has to be a considerable increase in the cross section for the production of $N\bar{N}$'s and also from the behaviour of the fractional hadron energy spectrum either the inelasticity or interaction mean free path or both have to change necessarily at very high energies compared to machine energies.

In this paper we present a discussion of the trends in the characteristics of interactions at ultra-high energies ($\gtrsim$ a few TeV) that reveal themselves when an attempt is made to adjust the parameters of high energy collisions in such a way that there is a better agreement between the expectations on the basis of Monte Carlo simulations and experimental results on high energy hadrons. In adjusting these parameters, we have been governed by the other properties of air showers also, like the size variation of the low energy hadrons and muons, and of the ultra-high energy muons and the relation between the primary energy and the shower size. Obviously such an adjustment is a synthetic one and cannot be claimed to be unique. It may turn out that all the changes

visualized are not strictly necessary or even that all of them may not be entirely sufficient and also all the properties of air showers may not be fully explained. In fact we find that while it has been possible to achieve, on the basis of these adjustments of parameters, a much closer agreement in certain properties and the right trends, regarding certain other properties discrepancies still remain, though they do not widen. The exercise has in the main shown that the directions in which changes are introduced are the right ones and calculations with further adjustment of parameters should result in a much better over-all agreement. To pursue further the adjustment of parameters, the limitation is really the computer time required, which is enormous. Also experimental results of much higher precision are necessary before further refinements of calculations are attempted.

2. Guidelines for adjustment of collision parameters

The experimentally observed features of high energy hadrons which have shown considerable departure from the predictions of simulations based on 'normal models' of high energy interactions are : (i) the hadron energy spectrum is very steep and there is evidence for a further steepening of the spectrum with increasing size ; (ii) the absolute numbers of hadrons observed experimentally are less by almost an order of magnitude ; (iii) the charged to neutral ratio of hadrons in EAS has a rather low value (~ 6) and decreases further (~ 3) at higher sizes ; (iv) the fractional hadron energy spectrum falls below the calculated spectrum of survivors and is different for different sizes.

While these features suggested the broad directions in which changes had to be introduced in collision parameters, it was necessary to go through a number of trial and iterative stages of calculations before a set of parameters could be arrived at, which, when adopted, gave a closer agreement between the Monte Carlo simulations and the experimental results. The steepening of the hadron spectrum at high energies suggested an increase of inelasticity and a reduction of the interaction mean free path. For energies up to 100 GeV, the study of the detailed cascade profiles of both charged and neutral induced hadron cascades in the multiplate cloud chamber had shown identical features and required an inelasticity less than 0·5 (Vatcha *et al* 1972). Since at these energies, the charged hadrons are mostly pions, this result also meant that at energies up to 100 GeV, the interactions of pions also should be treated as partially inelastic. A value of $\eta_N = \eta_\pi = 0{\cdot}35$ was therefore adopted. Since the steepening of the hadron spectrum was apparent from 100 GeV onwards and since the C/N ratio showed a rapid depletion of pions at energies greater than 200 GeV, both λ_π and η_π were radically changed over the narrow interval 10^{11} to 2×10^{11} eV. η_π was linearly increased from 0·35 to 0·9 and λ_π was decreased from 130 g cm^{-2} in air to 70 g cm^{-2}. In the case of nucleons it was not necessary to change the parameters over a narrow interval. The inelasticity of nucleons η_N was increased from 0·35 to 0·5 over the energy range 10^{11} to 10^{12} eV which is not in conflict with most of the experiments on hadrons in this energy range. η_N was further increased from 0·5 to 0·9 over the energy interval 10^{12} to 5×10^{14} eV and was held at this high value for higher energies. This increase was dictated by the consideration that the fractional hadron energy spectrum is different for showers of size less than and greater than 3×10^5. The interaction mean free path for nucleons λ_N was changed from 80 g cm^{-2} at $E < 10^{11}$ eV to 65 g cm^{-2} at $E \geqslant 10^{12}$ eV from similar considerations. It may be mentioned that there is some indication from the distribution of the points of interactions in the cloud chamber plates of cascades of energy greater than

10^{12} eV, for an interaction mean free path smaller than at lower energies. The proton satellite experiments of Akimov *et al* (1969) also show an increase in the cross section for proton–carbon interactions at energies greater than 6×10^{11} eV. From a comparison of the unaccompanied hadron energy spectra at various depths in the atmosphere Yodh *et al* (1972) have shown that the $\sigma_{\text{p-air}}$ (inelastic) increases from 250 mb at 10^{11} eV to 350 mb at $E \gtrsim 3 \times 10^{13}$ eV. These drastic changes in inelasticity and interaction mean free path resulted in the depletion of high energy muons and contradicted experimental observations unless a rapid increase of multiplicity was employed at very high energies. For this reason the multiplicity was taken at all energies to be proportional to $E^{1/2}$, since at lower energies it makes very little difference whether the multiplicity is ln E, $E^{1/4}$ or $E^{1/2}$, as far as the present calculations are concerned. A large multiplicity is indicated at ultra-high energies also because a rapid fragmentation of energy is expected at such energies. However, because of the rapid fractionation of energy, and to explain the rather slow rate of increase of high energy muons with shower size observed in the KGF experiments, it was necessary to reduce the probability of formation of isobars at $E > 10^{12}$ eV. When trials were made incorporating these changes it turned out that the relation between the primary energy and the shower size at the observational level was seriously affected. For a given primary energy the shower size was much too small compared to what was found by a direct comparison of the primary spectrum derived by the satellite experiment and the size spectrum determined at Ooty. In order to restore this relation it became essential to introduce a process similar to that of the gammaization process of Nikolsky (1967) according to which a considerable fraction of energy is transferred directly into the soft component by-passing pionization. The possibility of gammaization is also indicated from the feature of a rapid absorption of cascades of energies greater than 1 TeV which has been observed by Vatcha *et al* (1972).

The rather low value of the charge to neutral ratio observed by us for hadrons of energy greater than 25 GeV in showers of size greater than 3×10^5 when the number of hadrons is of the order of several hundred clearly demonstrates, as pointed out in the earlier paper, the presence of a large number of $N\bar{N}$'s among the hadrons. The time structure experiments of hadrons in air showers carried out at Ooty (Tonwar and Sreekantan 1971) have shown that there is a considerable increase in the cross section for the production of $N\bar{N}$'s at energies of the order of a few hundred GeV. There is confirmation for this trend from the recent ISR experiments. If such an increase in the cross section for the production of $N\bar{N}$'s is taken into account, then as shown by Murthy (1967) the rather low value of the C/N ratio can be explained even in conventional models of high energy interactions. However, our observation that this ratio decreases further to a value of $3{\cdot}2 \pm 0{\cdot}5$ in showers of size greater than 3×10^5 has very important implications and cannot be explained in the framework of the conventional models even taking into account increase of $N\bar{N}$ production. It is obvious that such a size dependent effect has to be traced to collisions which occur in showers of size greater than 3×10^5 and are not present in showers of smaller size, which means collisions of energy greater than about 5×10^{14} eV. Such high energy collisions take place only in the early stages of the hadron cascade and therefore high up in the atmosphere. In order to influence the C/N ratio of hadrons of energy as low as 25 GeV at 800 g cm^{-2} considering the very steep hadron energy spectrum, it is necessary that in these collisions a large fractionation of energy takes place and a large number of $N\bar{N}$'s of sufficient low energy are produced to take care of the attenuation in the intervening atmosphere. Under these circumstances the contribution to the hadrons from $N\bar{N}$'s produced in collisions of energy a few TeV and less turns out to be small even if we consider the increase in cross section. We have

therefore used the relations of the type

$$F_r = \frac{1}{1 + (4 \times 10^{14}/E)^3},$$

where E is the incident energy in eV,

$$F_i = \frac{7F_r}{1 + 6F_r},$$

where F_r is the fraction of $N\bar{N}$'s produced and F_i is the fraction of energy going into $N\bar{N}$'s in collisions of energy E.

Thus the parameters of high energy collisions for the final Monte Carlo simulations of the hadron cascades used are:

(i) *Inelasticity*

(*a*) Nucleons: $\eta_N = 0{\cdot}35$ for $E \leqslant 10^{11}$ eV
$= 0{\cdot}35$ to $0{\cdot}05$—linear rise for $E = 10^{11}$ to 10^{12} eV
$= 0{\cdot}5$ to $0{\cdot}9$—linear rise for $E = 10^{12}$ to 5×10^{14} eV
$= 0{\cdot}9$ for $E > 5 \times 10^{14}$ eV.

(*b*) Pions: $\eta_\pi = 0{\cdot}35$ for $E \leqslant 10^{11}$ eV
$= 0{\cdot}35$ to $0{\cdot}9$ linear rise for $E = 10^{11}$ to 2×10^{11} eV
$= 0{\cdot}9$ for $E > 2 \times 10^{11}$ eV.

(*c*) Fluctuations: If the average value is $\bar{\eta}$, the probability distribution is given by a sine function normalized between extreme values of $\frac{1}{2}(3\bar{\eta} - 1)$ to $\frac{1}{2}(\bar{\eta} + 1)$ corresponding to argument values of 0 and π of the sine function.

(ii) *Interaction mean free path*

Nucleons: $\lambda_N = 80$ g cm^{-2} for $E \leqslant 10^{11}$ eV
$= 80$ g cm^{-2} to 65 g cm^{-2}—linear decrease from $E = 10^{11}$ to 10^{12} eV
$= 65$ g cm^{-2} for $E > 10^{12}$ eV.

Pions: $\lambda_\pi = 130$ g cm^{-2} air for $E \leqslant 10^{11}$ eV
$= 130$ g cm^{-2} to 70 g cm^{-2}—linear decrease from 10^{11} to 2×10^{11} eV
$= 70$ g cm^{-2} for $E > 2 \times 10^{11}$ eV—fluctuations by Monte Carlo methods.

(iii) *Multiplicity*

In collisions of nucleons: $M_N = 2{\cdot}0 + 0{\cdot}2E^{1/2}$.
In collisions of pions: $M_\pi = 2{\cdot}0 + 0{\cdot}3E^{1/2}$.
Fluctuations are box type from $M/2$ to $3M/2$.

(iv) *Gammaization*

30% of available energy is distributed into 6 γ rays of equal energy on the average. The probability of gammaization increases from zero for $E \leqslant 10^{12}$ eV to 1 for $E \geqslant 10^{13}$ eV.

(v) *Isobar formation*

The probability of formation is 50% for $E \leqslant 10^{12}$ eV and decreases linearly to 0 at $E \geqslant 5 \times 10^{14}$ eV. When an isobar is formed, 20% of the total energy is available to a single fireball, and the remaining 80% is divided between a surviving nucleon (whose energy is determined by η_N) and three decay pions of equal energies on the average. The nucleon retains at least 16% of the total energy on the average even at the highest energies.

(vi) *Energy and p_T distribution of secondaries*
At $E > 8 \times 10^{14}$ eV there is equipartition of energy. At lower energies the same as Murthy *et al* (1968a, b).

(vii) *Nucleon–antinucleon production*
The fraction of $N\bar{N}$'s is given by

$$F_r = \frac{1}{1 + (4 \times 10^{14}/E)^3}$$

where E is the incident hadron energy in eV. The fraction of energy given to $N\bar{N}$ pairs is

$$F_i = \frac{7F_r}{1 + 6F_r}.$$

3. Results of Monte Carlo simulation and comparison with observation

In order to compare the results of simulations of EAS with experimental results, the simulated showers were generated from a primary energy spectrum from 10^{14} to 10^{16} eV and the resulting showers classified according to their size at 800 g cm^{-2} as in the experimental data. Full details are available in Vatcha (1972). The effects of a mixed composition have not been considered as the objective of the calculations is only to understand trends.

3.1. Relation between primary energy and shower size

The present calculations led to a conversion factor of 4·3 GeV per particle between the primary energy and the shower size at 800 g cm^{-2}. A value of about 2 Ge V per particle is obtained from a comparison between the primary energy spectrum directly measured in the proton satellite by Grigorov *et al* (1971) and the size spectrum measured by us at Ooty. Considering the uncertainties in flux due to solid angle factors which depend upon angular distribution of showers as well as the statistical errors in the determination of size etc, and also the uncertainties in the derivation of the primary spectrum in the satellite experiment, the discrepancy may not be very significant. The agreement can be improved by a readjustment of parameters especially the extent of gammaization, and energy fractionation.

3.2. Integral energy spectrum of hadrons in EAS

The integral energy spectrum of hadrons obtained on the basis of simulated showers is plotted in figure 1 corresponding to average weighted primary energy values of $1{\cdot}6 \times 10^5$ GeV, 5×10^5 GeV, $1{\cdot}6 \times 10^6$ GeV and 5×10^6 GeV. In the same figure the simulations of Murthy *et al* (1968a, b) and of Greider (1971) are also shown. The notations have been described in paper II. The experimental spectra obtained for the two size groups of $3{\cdot}2 \times 10^5$ or above and less than $3{\cdot}2 \times 10^5$ corresponding to average primary energies of 4×10^5 GeV and 3×10^6 GeV (using a conversion factor of 4·3 GeV/particle) are also shown. Even the lowest values given by Murthy *et al* for hadron numbers are larger than observed by at least an order of magnitude. The calculations of Greider give a slightly better agreement in number at energies of about 100 GeV or less, but because of the

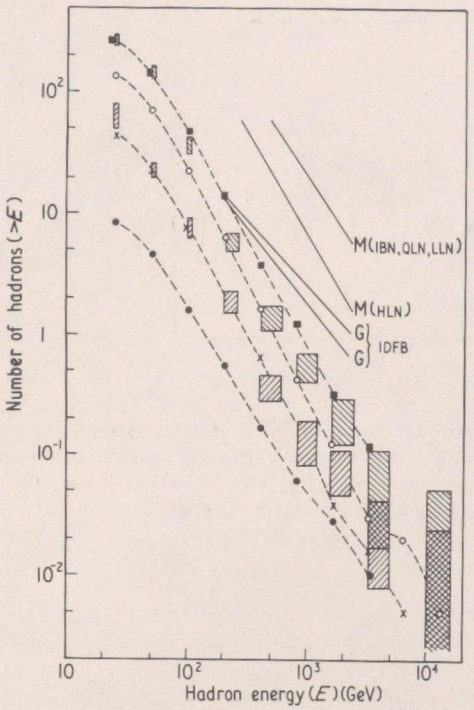

Figure 1. The integral energy spectrum of hadrons in EAS initiated by primaries of different energies. Average weighted primary energy values of $1{\cdot}6 \times 10^5$ GeV (●), $5{\cdot}0 \times 10^5$ GeV (×), $1{\cdot}6 \times 10^6$ GeV (○), $5{\cdot}0 \times 10^6$ GeV (■) are plotted. The results from the present Monte Carlo simulations indicate a steepening of the spectra with increasing primary energy. The results from the simulations of Murthy *et al* (curve M) and Greider (curve G) are also shown for primaries of energies of 10^6 GeV. The experimental values obtained from an earlier paper are also indicated: average weighted primary energy values of 3×10^6 GeV (▨) and 4×10^5 GeV (▨) are shown.

flatter spectrum the discrepancy increases at larger energies. There is fair agreement between experimental results and the predictions from the present calculations which also show the tendency for the energy spectrum to steepen with increasing primary energy.

In figure 2 the exponent γ of the integral energy spectrum of hadrons for different shower size groups is plotted and it is seen that the trend of steepening of the hadron spectrum with increasing size is reproduced to some extent although it is slower than experimental results indicate. This feature is a reflection of the hypothesis of strong energy fractionation at ultra-high energies with increasing dissipation of energy in the soft component, and can be adjusted further.

3.3. Size variation of the number of hadrons

In figure 3(*a*) the calculated number of hadrons for specific sizes is compared with experimental results shown by curves for different hadron energies. There is reasonable agreement at lower hadron energies but the calculated rate of increase of number is steeper than experimental ones especially at higher energies. The calculated rates are

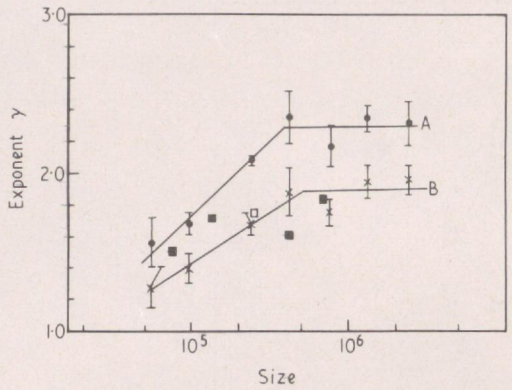

Figure 2. The variation of the exponent γ of the integral energy spectrum of hadrons with shower size in the range $E = 50-800$ GeV. The experimental curve A is obtained without considering the effects of systematic errors whereas the experimental curve B is obtained assuming maximum possible systematic errors. The points refer to the results of the present simulations.

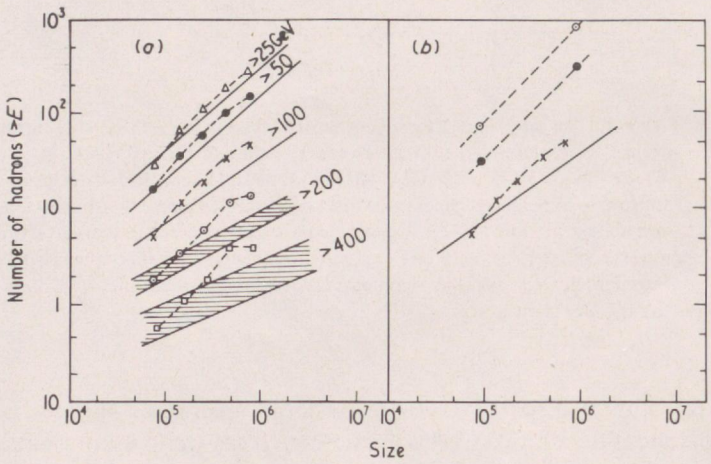

Figure 3. The variation of the number of hadrons of different threshold energies with shower size. The results of the present simulations are shown by points and the curves are obtained from experimental values given in an earlier paper. Figure 3(*a*) presents the results for hadrons with threshold energies from 25 GeV to 400 GeV. In figure 3(*b*) a comparison is made between the experimental results for hadrons of energies greater than 100 GeV (full line) with the present simulations ($\times$) as well as earlier simulations of Murty *et al* (○, without $N\overline{N}$, ⊙ with $N\overline{N}$).

slower for hadron energy thresholds of 800 GeV and 1600 GeV. It is significant that the present calculations give absolute numbers much closer to experimental numbers (within a factor of 2 at all hadron energies) than the previous calculations shown for hadrons of energy greater than 100 GeV in figure 3(*b*). The present calculations however do not indicate any break in the slope at a size of about 3×10^5 even for the highest hadron energies for which there is some experimental evidence.

3.4. The charge to neutral ratio of hadrons

In figure 4 the charge to neutral ratio obtained from the simulations as a function of energy for various size groups is plotted. The experimental points for two size groups (ie $\geqslant 3{\cdot}2 \times 10^5$ and $< 3{\cdot}2 \times 10^5$) are also shown. While the trend for the ratio to decrease

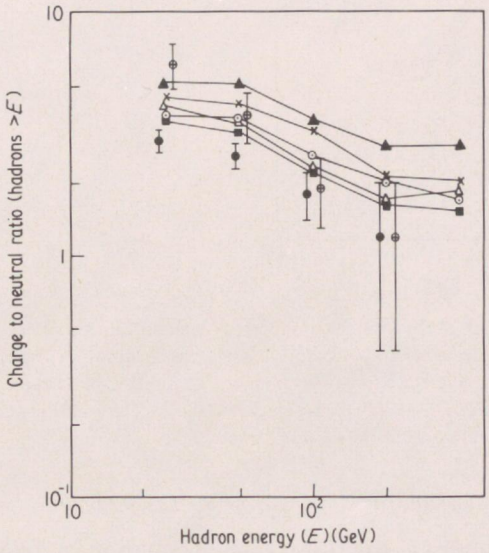

Figure 4. The variation of the charged to neutral ratio of hadrons with hadron energy for showers of different sizes. The five curves are obtained from the present simulations corresponding to different size groups: ▲ $5{\cdot}6 \times 10^4$–10^5; × 10^5–$1{\cdot}8 \times 10^5$; ⊙ $1{\cdot}8 \times 10^5$–$3{\cdot}2 \times 10^5$; △ $3{\cdot}2 \times 10^5$–$5{\cdot}7 \times 10^5$; ■ $5{\cdot}7 \times 10^5$–10^6. The experimental values for two size groups are also shown: ⧫ $> 3{\cdot}2 \times 10^5$; ⧫ $< 3{\cdot}2 \times 10^5$.

with increasing size is reproduced in the present calculations the values are slightly higher for energies greater than 100 GeV compared to the experimental values. The introduction of a small amount of $N\bar{N}$ production at energies of 1 TeV or less as discussed earlier would possibly reduce this discrepancy.

3.5. Variation of the number of muons with size

The calculated number of muons of different energy thresholds (ie 20 GeV, 220 GeV and 640 GeV) for different shower sizes are shown in figure 5. The experimental results of Sivaprasad (1971) with the KGF array for muons of energy greater than 220 and 640 GeV and those of Vernov *et al* (1968) for muons of energy greater than 20 GeV (extrapolated from > 10 GeV muons) are also shown. For low energy muons the agreement is reasonable whereas for high energy muons the calculated size variation is slightly steeper. However, for muons of energies of about 220 GeV or more, the discrepancy in the numbers at any size is less than 50%. The maximum discrepancy is in the number of muons of energy greater than 640 GeV at a size of the order of 10^5, which is a factor of three. These discrepancies could perhaps be reduced by further adjustments of parameters.

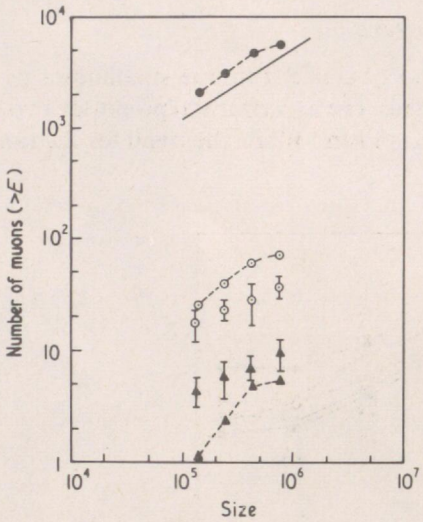

Figure 5. The variation of the number of muons of different threshold energies with shower size. The results of the present simulations are shown by points without error bars. The experimental points with error bars are for high energy muons obtained from the experiment at the Kolar gold fields: ⊙ > 220 GeV; ▲ > 640 GeV. The full line is the experimental curve slightly extrapolated from the data of Vernov *et al.*

3.6. The transverse momentum distribution of very high energy hadrons

In normal models of EAS development the transverse distribution of hadrons from the axis may be regarded as essentially determined by the height of the previous interaction with respect to the observational level and the transverse momentum acquired by the hadron in this interaction. This is because, in the normal models the number of hadrons that leak through from large heights without undergoing interactions is negligible, compared to those coming from interactions further down. In this case the transverse distribution of hadrons can be calculated without going through detailed Monte Carlo simulations. It is convenient to calculate the distribution of the parameter $Y = rE_0$ where r is the distance from the axis and E_0 is the energy of the hadron. The distribution of Y is the result of the distribution of the height of previous interaction and the distribution of the transverse momentum. Thus the differential distribution of 'Y' is given by

$$F(Y)\,\mathrm{d}Y = \int\int f(R)\,\mathrm{d}R\Phi(p_\mathrm{T})\,\mathrm{d}p_\mathrm{T}$$

subject to the condition $Y = rE_0 = p_\mathrm{T}R$, where r is the distance of the hadron from the core, E_0 is the hadron energy, R is the distance from the last interaction to the observation level and p_T is the transverse momentum given to the hadron. The distribution of R is given by

$$f(R)\,\mathrm{d}R = \mathrm{e}^{-X/\lambda}\frac{\mathrm{d}X}{\lambda}$$

where λ is the hadron interaction mean free path and X is the amount of matter equivalent to the distance R. The distribution of p_T is assumed to be

$$\Phi(p_\mathrm{T})\,\mathrm{d}p_\mathrm{T} = \frac{p_\mathrm{T}}{p_0}\exp\left(-\frac{p_\mathrm{T}}{p_0}\right)\frac{\mathrm{d}p_\mathrm{T}}{p_0}.$$

Then

$$F(Y)\,dY = dY\int_0^\infty f\left(\frac{Y}{p_T}\right)\exp\left(-\frac{p_T}{p_0}\right)\frac{dp_T}{p_0^2}.$$

Using the relation† $X = G - X_0\exp[-\{(R+H)/Z_0\}]$ between X (g cm^{-2}) and R (km), where X_0, Z_0 and G are constants, the differential distribution of Y reduces to the form

$$F(Y)\,dY = dY\frac{X_0}{\lambda Z_0 p_0^2}\int_0^\infty \exp\left(-\left[\frac{G}{\lambda}+\frac{Y+p_T H}{Z_0 p_T}+\frac{p_T}{p_0}-\frac{X_0}{\lambda}\exp\left\{-\left(\frac{Y+p_T H}{p_T Z_0}\right)\right\}\right]\right)dp_T$$

where $X_0 = 1075\,\text{g cm}^{-2}$, $Z_0 = 7{\cdot}5\,\text{km}$, $G = 800\,\text{g cm}^{-2}$, $\lambda = 80\,\text{g cm}^{-2}$ and $H = 2{\cdot}2\,\text{km}$.

In figure 6 the expected distribution of Y is plotted for $p_0 = 0{\cdot}25$, 1·0, 5·0 as curves A, B, and C from the above calculations.

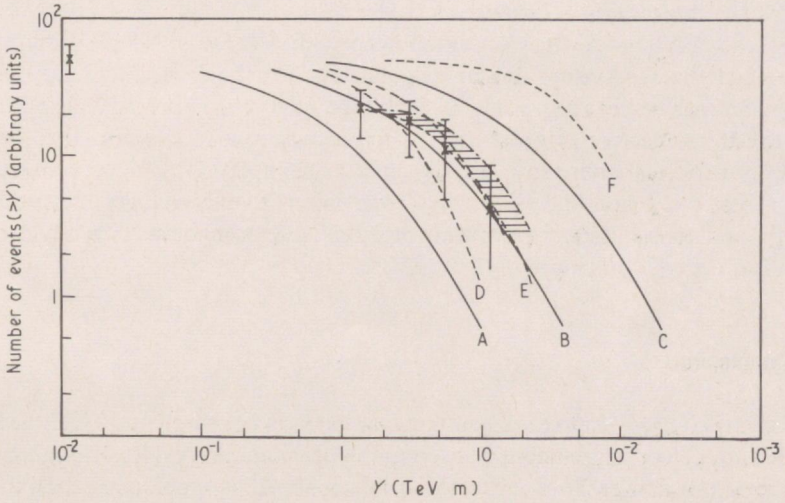

Figure 6. The lateral distribution of cascades of energy greater than 1 TeV associated with EAS. The variable Y is the product of the cascade energy (TeV) and its distance from the shower core (m). The curves A, B and C are obtained for different average p_T values (0·5, 2·0, 10·0 GeV/c respectively) based upon calculations assuming a normal development of EAS. The curves D, E and F are similar curves for average p_T values (0·5, 2·5, 10·0 GeV/c respectively) obtained from the present simulations. The experimental points which are also shown as well as all the curves are normalized at $Y = 0$.

In our case, when we have radically changed the parameters of collisions and introduced large fractionation of energy in the first few collisions at the top of the atmosphere, most of the high energy hadrons at the observational level are due to 'leak throughs' from various levels and especially from the first few interactions in the atmosphere. Because of this reason, it is necessary to obtain the distribution of the transverse displacement or alternatively of the parameter Y only through detailed Monte Carlo simulations. The curves D, E and F in figure 6 are those obtained from such Monte Carlo calculations for primaries in the energy range 10^6–$3{\cdot}2\times10^6$ GeV, weighted according to the primary spectrum. All the curves are normalized at $Y = 0$.

It is seen from figure 6 in which the experimentally obtained distribution of Y is also given for TeV cascades (table 1 of paper I), that in the normal models, the closer

† This approximate relation is obtained from the curve given by Rossi (1965) near the depth of 800 g cm^{-2}.

fit to the experimental points is given by curve B which corresponds to a $\langle p_T \rangle$ value of 2·0 GeV/c, rather than curve A which corresponds to the usually accepted value of 0·5 GeV. However, according to our calculations in which the interaction characteristics are radically different, within errors even the value of 0·5 GeV/c could be accommodated.

In paper II we have seen that the absolute number of high energy hadrons obtained in our experiment is lower than the numbers obtained in other experiments. We would like to remark at this stage that if this difference is attributed to any systematic underestimate of energies, say, by a factor of five, then the experimental distribution of figure 6 would move to the right by this factor and would indicate a mean average transverse momentum of 10 GeV/c even in a normal model of strong interactions. Thus any systematic bias in the hadron energy estimate, if it exists at all, cannot be used to explain away all the changes in the interaction characteristics which have been introduced at ultra-high energies; either $\langle p_T \rangle$ increases very drastically or the inelasticity increases and/or the interaction mean free path decreases.

A reasonably good fit is obtained even with a value of 0·5 GeV/c for $\langle p_T \rangle$ because of the fact that according to our calculations, for the reasons already discussed, high energy hadrons essentially come as 'leak throughs' from higher levels of the atmosphere and are thus effectively spread out. Such a picture also explains the observation that the C/N ratio for hadrons of energy greater than 100 GeV decreases from a value of $2{\cdot}3 \pm 0{\cdot}5$ at $r < 8$ m to $1{\cdot}3 \pm 0{\cdot}5$ at $r > 8$ m since the effective production height of high energy nucleons is higher than that of pions, due to enhanced production of $N\bar{N}$'s in ultra-high energy collisions.

4. Conclusions

It is clear from § 3 that the adjustment of various parameters of high energy collisions has led to a closer agreement between the experimental results on high energy hadrons and muons and the Monte Carlo simulations. It is significant that this adjustment which is mainly guided by the behaviour of the high energy hadrons and muons has not led to any serious contradictions with respect to other properties of air showers. While it is clear that with further adjustment of parameters and more intensive calculations it may become feasible to bring much closer agreement, it is not warranted at the present stage considering the available accuracy of the experimental results. What can be claimed at this stage is that the various changes introduced may be inaccurate in detail, but the general trend is in the right direction. The over-all picture regarding the behaviour of ultra-high energy interactions and the development of hadronic cascades in the atmosphere that emerge from the present study may be stated as follows.

At energies less than 100 GeV, the hadron interactions are only partially inelastic. A large fraction of the energy is still maintained in a 'surviving' hadron which emerges often in an excited isobaric state. As the energy approaches the TeV region, the inelasticity increases slightly and the cross section also increases as more channels become available for interaction. Nucleon–antinucleon pair production starts becoming important at these energies. At the same time, a considerable fraction of the available energy is occasionally given to the soft component by-passing pionization; the probability of this 'gammaization' component (a terminology introduced by Nikolsky) increases with energy. As the energy increases still further the probability of isobar formation reduces so that large fractions of energy are not available to a few secondaries. At the highest energies of about 5×10^5 GeV or more, strong energy fractionation takes

place and isobar formation is not significant. As the inelasticity increases, the fraction of energy available to 'gammaization' also increases. A drastic increase in the production of nucleon–antinucleon pairs occurs around the same energy, and long before this energy is reached, the multiplicity increases proportional to $E^{1/2}$. However, any apparent increase in $\langle p_T \rangle$ at such energies inferred from EAS data is explicable on the basis of an increase in the level of production of high energy hadrons rather than an actual increase in the value of $\langle p_T \rangle$.

References

Akimov V V *et al* 1969 *Proc. 11th Int. Conf. on Cosmic Rays, Budapest* 1969 vol 3 (Budapest: Central Research Institute for Physics) pp 211–4

Greider P K F 1971, *Proc. 12th Int. Conf. on Cosmic Rays, Hobart* 1971 vol 3 (Hobart: University of Tasmania) pp 970–5, 976–81

Grigorov N L *et al* 1971 *Proc. 12th Int. Conf. on Cosmic Rays, Hobart* 1971 vol 5 (Hobart: University of Tasmania) pp 1746–51

Murthy G T 1967 *PhD Thesis* University of Bombay

Murthy G T *et al.* 1968a *Can. J. Phys.* **46** S147–52

—— 1968b *Can. J. Phys.* **46** S159–63

Nikolsky S I 1967 *Sov. Phys.–JETP* **24** 535–45

Rossi B 1965 *High Energy Particles* (New York: Prentice-Hall) p 545

Sivaprasad K 1971 *PhD Thesis* University of Bombay

Tonwar S C and Sreekantan B V 1971 *J. Phys.* A: *Gen. Phys.* **4** 868–82

Vatcha R H 1972 *PhD Thesis* University of Bombay

Vatcha R H and Sreekantan B V 1973a *J. Phys.* A: *Math., Nucl. Gen.* **6** 1050–66

—— 1973b *J. Phys.* A: *Math., Nucl. Gen.* **6** 1067–77

Vatcha R H, Sreekantan B V and Tonwar S C 1972 *J. Phys.* A: *Gen. Phys.* **5** 859–76

Vernov S N *et al* 1968 *Can. J Phys.* **46** S197–200

Yodh G B, Pal Y and Trefil J S 1972 *Phys. Rev. Lett.* **28** 1005–8